



Fermi National Accelerator Laboratory

FSUHEP-920214
IIT-92-05

FERMILAB-PUB-92/59-T

Parton Distribution Functions of Hadrons*

Joseph F. Owens[†]

Physics Department, Florida State University
Tallahassee, Florida 32306

Wu-Ki Tung[‡]

Physics Department, Illinois Institute of Technology
Chicago, Illinois 60616

and

Fermi National Accelerator Laboratory
Batavia, Illinois 60510

March 12, 1992

Abstract

The QCD analysis of parton distribution functions in hadrons is reviewed. Elements of perturbative QCD which form the basis of this analysis and recent developments on the various physical processes which contribute most significantly to the global analysis are summarized. The theoretical, experimental, and phenomenological issues and uncertainties involved in a comprehensive study of parton distributions needed for contemporary precision QCD applications and high energy predictions are discussed in some detail. The status of currently available distribution sets and their proper use are examined. Finally, a list of yet-to-be finished tasks and critical challenges in this key area of high energy physics research is presented.

*To be published in Annual reviews of Nuclear and Particle Science.

[†]Supported in part by the United States Department of Energy and the Texas National Laboratory Research Commission.

[‡]Supported in part by the National Science Foundation and the Texas National Laboratory Research Commission.



1 Introduction

The standard model (SM) has undergone a great deal of development in both the electroweak [1] and the strong interaction [2] sectors during the past two decades. On both frontiers, current research focuses on issues of precision and consistency far beyond those possible in the qualitative leading order picture of the 1970's. Precision studies of the SM provide, on the one hand, ever-improving determinations of the unknown parameters of the theory and, on the other hand, a window into new physics beyond the minimal theory. These two aspects are, indeed, completely inseparable.

Quantum Chromodynamics (QCD) is a theory of interacting quarks and gluons and provides the basic description of strong interactions in the standard model. The quarks also interact with leptons and vector bosons via the electroweak force. However, physical processes involve only leptons, vector bosons and hadrons. In order to make meaningful comparisons between theory and experiment, we need a formalism which relates calculable (elementary) quantities to measurable (physical) ones. For high energy processes, perturbative QCD provides this framework through “factorization theorems”: physical cross-sections are factorized, to all orders of the QCD running coupling α_s , into a “hard cross-section” among elementary partons and a “soft part” consisting of universal distribution functions of partons inside hadrons. In leading order (LO), or tree-approximation, this formalism reduces to the simple parton model of the earlier years. We have, however, progressed far beyond that.

The universal (*i.e.*, process-independent) parton distribution functions (PDF) play a central role in SM phenomenology. Many of the most precise tests of the electroweak theory are currently limited by the lack of reliable PDF. All quantitative calculations for signals of “new physics” at high energies, as well as standard model processes (which form significant backgrounds for the new physics), depend on our current knowledge of the PDF. Most lepton-hadron and hadron-hadron scattering processes can serve either as a source of information on the PDF, or as testing grounds of QCD predictions based on known PDF. The systematic analysis of these processes to extract accurate parton distributions is therefore intrinsically intertwined with all aspects of high energy physics research.

The relatively simple first generation of PDF no longer satisfy the rigorous demands of current applications. As both theory and experiments have made significant progress in the level of sophistication and complexity, the second and third generation parton distribution analyses necessarily involve many non-trivial issues and uncertainties. Not all of these are fully taken into account in currently used PDF. Many of the subtleties are also unfamiliar or unknown to the average user of these PDF.

The purpose of this article is to: (i) summarize the elements of perturbative QCD which form the basis of parton distribution analysis (Secs. 2 and 3); (ii) review the various physical processes which contribute most significantly to this analysis (Sec. 4); (iii) describe the strategies for global analysis of parton distributions and discuss in some detail the theoretical, experimental, and phenomenological issues and uncertainties involved in the global analysis (Sec. 5); (iv) comment on the currently available distribution sets and their proper use (Sec. 6); and (v) conclude with a list of unfinished tasks and critical challenges for further progress in this key area of high

energy physics research (Sec. 7).

Due to space limitations, for well-established results we shall only briefly summarize the most relevant elements and, wherever appropriate, refer the reader to available books and review articles for comprehensive lists of references to the original papers. Additional details on many of the topics to be discussed in this review can be found in the papers in [3].

2 QCD Formalism for Hard Processes

2.1 Factorization Theorems and the Parton Model

In the original parton model, hard-scattering cross-sections are written as the product of two probabilities: parton distribution functions (the probability of finding partons of a given flavor and momentum fraction inside the hadron) and the parton level cross sections (the probability for the hard scattering subprocess to occur). With the advent of QCD, the fundamental ideas underlying the parton model received theoretical support through the systematic study of the short distance behavior of quark and gluon scattering cross sections using perturbative techniques. When the lowest order expressions of these cross sections are used, one reproduces the simple parton model.

When higher order terms are included, one encounters divergences which must be regularized (rendered finite) and properly subtracted (renormalized) in order to yield meaningful finite results. The systematic subtraction of ultraviolet singularities leads to the introduction of a running coupling α_s (to be discussed in the next section) which depends on a *renormalization scale* μ . Since $\alpha_s(\mu)$ becomes small for large μ (asymptotic freedom), we obtain a small expansion parameter by choosing μ to be of the order of a large characteristic momentum transfer in the scattering process. This justifies the use of the perturbative approach for such hard processes. In the limit of zero-mass partons, which is appropriate for leading power-law (*i.e.*, twist-2) analysis, one also encounters collinear divergences. Physically, the subtraction of collinear divergences corresponds to removing the overlap (hence the double-counting) between that part of the next order cross-sections with almost collinear and on-mass-shell lines and the contribution of the corresponding lower order term. The subtracted higher order correction is ambiguous by a finite amount, depending on how much of the unsubtracted result is reclassified as part of the lower order term. The systematic treatment of this problem to all orders leads to the concept of parton distribution functions which depend on a *factorization scale*. This factorization scale serves to separate the short- and long-distance portions of the scattering process; therefore, it should also be of the same order of magnitude as the characteristic large momentum scale of the physical process. Since the factorization and renormalization scales have distinct origins, they need not be exactly the same. However, they have to be of the same order of magnitude in order to avoid logarithms of large ratios. For simplicity, in subsequent discussions we shall use the symbol μ for both scales and do not attempt to distinguish the two unless necessary.

The precise results of the systematic analysis of the high energy behavior of hard cross-sections are expressed in a set of *factorization theorems*. They provide the theoretical basis of the QCD parton formalism. For comprehensive recent reviews, see Refs. [4] and [5]. We quote only the most useful results.

For a generic lepton-hadron scattering process $\ell + A \longrightarrow \ell' + C + X$ where C either represents an identified final-state particle with specific attributes (such as heavy mass or large transverse momentum) or is null in the case of total inclusive scattering, the factorization formula for the cross-section (excluding the known lepton vertex) reads:

$$\sigma_{A \rightarrow C}^i(q, p) = \sum_a \int_x^1 d\xi f_A^a(\xi, \mu) \hat{\sigma}_{a \rightarrow C}^i(q, \xi p, \mu, \alpha_s) \quad (1)$$

where A is the target hadron label, a is the parton label, i is the electroweak vector boson (weak isospin and helicity) label, (q, p) are the momenta of the vector boson and the hadron respectively, μ is the renormalization scale, and ξ is the fractional momentum carried by the parton with respect to the hadron. This basic theorem expresses the physically measurable cross-section as a convolution of a set of universal parton distribution functions f_A^a and a hard-scattering cross section $\hat{\sigma}_{a \rightarrow C}^i$.

Similarly, for a generic hard hadron-hadron collision process $A + B \rightarrow C + X$, the corresponding factorization theorem, when applicable [4, 5], states:

$$\begin{aligned} \sigma_{AB \rightarrow C}(p_A, p_B, p_C, \dots) = \\ \sum_{a,b} \int_{x_a}^1 d\xi_a \int_{x_b}^1 d\xi_b f_A^a(\xi_a, \mu) \hat{\sigma}_{ab \rightarrow C}(\xi_a p_A, \xi_b p_B, \mu, \alpha_s) f_B^b(\xi_b, \mu) \end{aligned} \quad (2)$$

where ξ_a and ξ_b represent the fraction of momenta carried by the two partons with respect to the two incoming hadrons, $\hat{\sigma}_{ab \rightarrow C}$ represents the cross-section of the fundamental parton process $a + b \rightarrow C + X$, and x_a and x_b represent appropriate integration limits set by the kinematics of the process under consideration.

2.2 Renormalization Scheme- and Scale-Dependence

The factorization theorems hold to all orders in α_s ; they are only subjected to power-law (higher-twist) corrections. It is important to note that the physical cross-sections on the left-hand sides of the factorization theorems are independent of the renormalization scheme and the choice of the scale μ (both needed to define the renormalized hard cross-section $\hat{\sigma}$) as they are artifices of the perturbative approach. Thus, the *scheme-* and *scale-dependence* of $\hat{\sigma}$ on the right-hand sides of these equations must be compensated by corresponding dependences of the parton distribution functions. This is the formal origin of the scheme- and scale-dependence of parton distributions. In particular, a change in the factorization scale μ merely amounts to reshuffling finite contributions between $\hat{\sigma}$ and $f_A^a(x, \mu)$ – due to shifting the boundary which defines collinear and non-collinear parton lines, as mentioned earlier. Thus, parton distribution functions are theoretical constructs which are *not* “physical” (in the sense that they are unambiguously and directly measurable) as they are often perceived to be.

Truncating the perturbation series at a given order spoils the perfect compensation between the scale-dependences of $\hat{\sigma}$ and $f_A^a(x, \mu)$, and hence introduces an

artificial dependence on the choice of μ to the QCD prediction for the cross-section. This represents an intrinsic uncertainty of the perturbative approach which must be understood and brought under control in quantitative applications.

The leading-order (LO) QCD formalism consists of using the tree-level results for the hard cross-section, the one-loop expression for the running coupling (Sec. 2.3), and parton distributions generated by one-loop evolution kernels (Sec. 3.1). This formalism provides a remarkably consistent description of a wide variety of large momentum transfer processes – see Ref. [6] for a review. However, at this level of approximation, the hard-cross-section has no μ -dependence (except through a possible overall power of $\alpha_s(\mu)$, depending on the process) so that the cross-section acquires a net μ -dependence through $f_A^a(x, \mu)$. As the scale is not specified other than that it should be of the order of a large momentum variable, the predictions will vary over a considerable range when the choice of this variable or the proportionality constant between μ and this variable is changed. For instance, if the relevant region of x in the parton distributions is above about 0.2, the predictions become monotonically decreasing functions of the scale. Reasonable variations in the choice of μ , *e.g.*, $p_T/2$ or $2p_T$ in high- p_T processes, can cause the predictions to vary by a factor of two or more.

A related problem is that the scale parameter Λ in the running coupling (see Sec. 2.3) is, strictly speaking, not well-defined in LO calculations: changing its value by any finite factor only leads to corrections of the next order, and hence can be ignored! Likewise, changes in the factorization prescription affect only subleading terms and, hence, can be made freely. All these, however, result in different numerical predictions. In summary, the LO formalism suffers from rather severe artificial factorization scheme- and scale-dependence which limit its usefulness as a quantitative model of high energy processes.

The next-to-leading order (NLO) formalism – involving NLO hard cross-sections with 2-loop α_s and 2-loop-evolved parton distributions – greatly improves the situation. All three elements now acquire unambiguous meaning, and the net scale dependence of the predictions on physical cross-sections is substantially reduced because the variation in one of these factors will be compensated by the others (except for even higher order corrections). This compensation is guaranteed by theory (the renormalization group equation)—provided consistency in the choice of renormalization and factorization schemes and scales is maintained in handling all elements of the calculation. This proviso is crucial because any mixed use of these quantities defined in different schemes (implicitly or explicitly) spoils the cancellation mechanism and, hence, gives results no better than the LO formalism.

We conclude therefore: (i) quantitative applications of the QCD-parton formalism require at least the NLO approximation; and (ii) at NLO, it is essential to explicitly specify the choice of renormalization and factorization scheme for both $\hat{\sigma}$ and $f_A^a(x, \mu)$, and to maintain the consistency of these. Disregarding this essential feature of the factorization theorem inevitably leads to misleading results. For instance, it has been pointed out recently that the scheme-dependence of the gluon and sea-quark distributions can be quite substantial [7]. This can lead to important phenomenological consequences (*cf.* Sec. 6).

2.3 The QCD Coupling and Λ_{QCD}

The running coupling $\alpha_s(\mu)$ is the most basic of QCD quantities. We examine some non-trivial aspects of the QCD coupling function α_s in the presence of heavy quarks. To begin, we recall the standard formulas for α_s in LO and in NLO in the case of all zero-mass quarks:

$$\alpha^{LO}(n_f, \mu/\Lambda) = \frac{4\pi}{\beta_0 \log(\mu/\Lambda)^2} \quad (3)$$

$$\alpha^{NLO}(n_f, \mu/\Lambda) = \frac{4\pi}{\beta_0 \log(\mu/\Lambda)^2} \left[1 - \frac{\beta_1}{\beta_0^2} \frac{\log \log(\mu/\Lambda)^2}{\log(\mu/\Lambda)^2} \right] \quad (4)$$

where n_f is the number of (massless) quark flavors and it enters the right-hand side through the constants,

$$\beta_0 = \frac{33 - 2n_f}{3} \quad \beta_1 = 102 - \frac{38n_f}{3} \quad (5)$$

If all quarks are massless, the number n_f is fixed and the running coupling α_s is determined by a single parameter Λ – the “QCD lambda”. In the presence of massive quarks, the situation is quite different. According to the decoupling theorem [8], each heavy quark i with mass m_i is effectively decoupled from physical cross-sections at energy scales μ below a certain threshold Q_i which is of the order m_i . Thus, the number of effective quark flavors n_f^{eff} is an increasing step function of the scale μ . Under this circumstance, the specification of the running coupling α_s and the associated Λ_{QCD} is not as simple as before. Although this point is fairly well-known, there still exists confusing and ambiguous statements about these parameters in the current literature and in conference presentations. Hence, it is worthwhile to summarize the proper formulation of the problem explicitly.

The definitions of α_s and Λ_{QCD} in the presence of mass thresholds are not unique – they are renormalization-scheme dependent. A *natural* choice is based on the requirement that $\alpha_s(\mu)$ be a continuous function of μ , and that between thresholds, it reduces to the familiar \overline{MS} α_s [9]. This requirement leads to the condition that $Q_i = m_i$ (in contrast to $2m_i$, or even $4m_i$, as are often used). This choice has the additional desirable feature that the parton distribution functions so defined are also required to be continuous across the thresholds. If Eq. (4) is to remain valid with α_s being continuous in μ , but n_f a discontinuous function of μ , it is quite obvious that the effective value of Λ must also make discontinuous jumps with μ at heavy quark thresholds. The same remark applies if one uses the LO formula for α_s , Eq. (3).

Figure 1a shows a typical α_s vs. μ plot; and Figure 1b shows the corresponding Λ_{QCD} as a function of μ (bottom scale) and n_f^{eff} (top scale). Figure 1a explicitly shows that the running coupling function of QCD $\alpha_s(\mu)$ can be unambiguously specified by giving its value at a (standard) scale, say M_Z . On the other hand, as shown in Figure 1b, this same coupling function is associated with many different values of Λ_{QCD} , depending on the number of effective quark flavors and on whether the LO or NLO formula is used. Thus, if one prefers to define α_s by specifying a value of Λ_{QCD} , it is imperative that one specifies the associated n_f^{eff} and the order (LO or

NLO) explicitly. In the recent literature, the second-order $\overline{\text{MS}}$ Λ_{QCD} with 4 flavors has increasingly become the standard choice, although that with 5 flavors is also used – too often without explicit notation.

3 Parton Distribution Functions

3.1 QCD Evolution Equations

The scale dependence of the parton distributions in QCD is generated by the interactions of the quarks and gluons via such elementary processes as gluon emission from quarks, $q \rightarrow qg$, gluon emission by gluons, $g \rightarrow gg$, and the creation of quark-antiquark pairs by gluons, $g \rightarrow q\bar{q}$. Consider deep inelastic scattering where one of the quarks in the target nucleon interacts with the relevant electroweak current. This quark may have radiated gluons either prior to or subsequent to the interaction or it may have originated from a gluon. In any case, the unobserved radiated partons must be integrated over the remaining available phase space, the scale for which is set by μ . These radiative corrections are the physical source of the logarithmic scale dependence predicted by the theory. More precisely, the scale dependence of the parton distributions are governed by a set of coupled integro-differential QCD-evolution equations, valid to all orders in α_s [10, 11]

$$\frac{df^q(x, \mu)}{dt} = \frac{\alpha_s(\mu)}{2\pi} \int_x^1 \frac{dy}{y} \left[P_{qq}(y) f^q\left(\frac{x}{y}, \mu\right) + P_{qg}(y) f^g\left(\frac{x}{y}, \mu\right) \right] \quad (6)$$

$$\frac{df^g(x, \mu)}{dt} = \frac{\alpha_s(\mu)}{2\pi} \int_x^1 \frac{dy}{y} \left[\sum_q P_{gq}(y) f^q\left(\frac{x}{y}, \mu\right) + P_{gg}(y) f^g\left(\frac{x}{y}, \mu\right) \right] \quad (7)$$

where $t = \ln(\mu^2/\Lambda^2)$, and the superscript q is used to denote quark flavors. The kernels of these equations, $P_{ij}(z)$, correspond to splitting functions for the elementary processes mentioned before and have the physical interpretation as the probability density for obtaining a parton of type i from one of type j with a fraction z of the parent parton's momentum.

In LO (1-loop) QCD there are four such splitting functions. They can be found in all standard books and references. The NLO (2-loop) expressions for $P_{ij}(z)$ was calculated by several groups [12]–[15]. Up until recently, there had been an unresolved minor discrepancy for part of the function P_{gg} between the results obtained in a covariant gauge and those obtained using the axial gauge. This has now been clarified: a detail discussion can be found in [16].

When solving this coupled set of equations it is convenient to define a singlet distribution

$$\Sigma(x, \mu) = \sum_q \left[f^q(x, \mu) + f^{\bar{q}}(x, \mu) \right] \quad (8)$$

which mixes with the gluon in two coupled evolution equations of the form given above.

The nonsinglet (or valence) distributions

$$f^{q*}(x, \mu) = f^q(x, \mu) - f^{\bar{q}}(x, \mu) \quad (9)$$

each satisfy an uncoupled equation. In LO, the kernel of this equation is simply the well-known splitting function $P_{qq}(z)$. Beyond LO, in addition to higher order term for $P_{ij}(z)$, there emerges another type of non-singlet distribution:

$$f_+^{q*}(x, \mu) = f^q(x, \mu) + f^{\bar{q}}(x, \mu) - \Sigma(x, \mu)/n_f^{eff}. \quad (10)$$

which also satisfies an uncoupled equation with a different kernel function [12]–[15].

This set of equations can be solved numerically, once a set of distributions is specified at some initial value of μ , hereafter denoted by μ_0 . Note that in each case the logarithmic derivative with respect to μ at a given value of x is given in terms of the parton distributions evaluated at the same value of μ with momentum fractions greater than or equal to x . This is of practical interest since experimental measurements at fixed μ and beam energy can not reach all the way to $x = 0$.

3.2 Systematics of Scale Dependence

The scale dependence of parton distributions has the general feature that $f(x, \mu)$ is a decreasing function of μ at large values of x , and it becomes an increasing function at small x [17]. This can be understood mathematically by considering the LO non-singlet evolution equation as described above. Substituting in the expression for P_{qq} in the uncoupled equation yields

$$\begin{aligned} \frac{df^{q*}(x, \mu)}{d\ln\mu} = & \frac{\alpha_s(\mu)}{2\pi} C_F \int_x^1 \frac{dy}{y(1-y)} \left[(1+y^2)f^{q*}\left(\frac{x}{y}, \mu\right) - 2yf^{q*}(x, \mu) \right] \\ & + \frac{\alpha_s(\mu)}{2\pi} C_F \left[\frac{3}{2} + 2\ln(1-x) \right] f^{q*}(x, \mu) \end{aligned} \quad (11)$$

The first term in Eq. (11) is negative for all x (since $f^{q*}(x, \mu)$ is a decreasing function of x and the argument of the second term is always smaller than that of the first term) while the second is negative at large x , becoming positive for $x \leq 1 - \exp^{-\frac{3}{2}} \approx 0.53$. Therefore, at large values of x , $f^{q*}(x, \mu)$ decreases with increasing μ . On the other hand, the integral of f^{q*} on x from 0 to 1 must remain constant as μ varies because it counts the net number of valence quarks of a given type (the quark-number sum rule). Thus, $f^{q*}(x, \mu)$ must increase with μ at small x to compensate for the decrease at large x . The physics behind this pattern of scaling violation is simple to understand. A parton with a given momentum fraction x can radiate another parton, thereby decreasing its momentum fraction and reducing the value of the parton density at that value of x . However, the parton density at that value of x will also receive an increase from partons with higher momentum fractions radiating partons. There is thus a type of gain-loss competition taking place. Indeed, it is possible to recast the derivation of the LO evolution equations into such a form, thereby making the gain-loss terms manifest [18].

The preceding discussion illustrates a general feature of the μ dependence of the parton distributions, namely that the values of the distributions at small x and large μ values are determined in large part by the values of the distributions at large x and small μ values. Thus, a significant fraction of the region of x and μ which is relevant for predictions for high energy collider processes receives contributions via the evolution equations from regions which are well measured by current experiments. This feature has made it possible to generate reliable predictions for many processes in new energy regimes.

3.3 Extrapolations to Small x

For a high energy process, the most relevant range of x values is given by $x \sim \mu/\sqrt{s}$ where μ is a typical momentum scale and \sqrt{s} is the center-of-mass energy. At future high energy colliders where \sqrt{s} will be very large, many interesting physics processes taking place at moderate values of μ , say 5 – 50 GeV, will probe parton distributions and interactions at very low values of x . In hadron colliders, processes such as the production of minijets (jets with moderate values of p_T), heavy-flavor (mainly B -mesons), and low-mass lepton-pairs all belong to this category. The behavior of parton distributions in this region is not well understood for the following reasons: (i) theoretically, within the perturbative QCD framework, the occurrence of powers of $\log(1/x)$ (which becomes large in this region) can spoil the conventional (twist-2) formalism as described up to now; (ii) phenomenologically, even within the standard approach, the initial parton distributions needed in solving the evolution equation are largely unknown because no existing data extend into this region. Unfortunately, for moderate values of μ , as we have here, the solutions to the evolution equation are sensitive to the initial distributions, unlike at large μ where their behavior is primarily driven by the leading singularity of the evolution kernel at $x = 0$.

The theoretical issues can be further differentiated into several fronts: (i) For fixed μ , the small x limit is analogous to the Regge limit in hadronic processes ($s \rightarrow \infty$) for which there exists certain conventional wisdom and a large amount of more recent QCD study [19] pioneered by the work of Lipatov [20]. In particular, the Lipatov Equation [20] (involving resummation of large $\log(1/x)$ factors to all orders) and its recent generalizations [21] govern the “small- x evolution” of parton distributions for fixed μ ; (ii) In the region where both $\log(\mu/\Lambda)$ and $\log(1/x)$ are large, a different set of resummation techniques has to be developed. The large body of work on this topic has been summarized in several recent comprehensive reviews [22]; and (iii) Since the parton densities increase precipitously as $x \rightarrow 0$, they will eventually saturate at some value of x when the packed partons become so dense that they interact strongly in spite of the small effective coupling [22, 23]. In the saturation region, the parton picture itself breaks down; one enters an entirely new regime of QCD. All these three fronts present new challenges for theorists. Much progress has been made in the last ten years in developing new techniques of calculation in these regions, but they are not yet at a stage ready for routine applications. We refer interested readers to [19] for state-of-the-art reviews on this active frontier of research.

All phenomenological analyses of parton distributions based on the usual QCD

formalism use certain assumed parametrizations of the initial distribution functions which implicitly determine the extrapolated small- x behavior. The conventional ansatz of a power law behavior $f(x, \mu_0) \sim x^\gamma$ as $x \rightarrow 0$ for the gluon and sea quarks with γ ranging from -1 (Regge “Pomeron”) to -1.5 [24] is a highly ambiguous proposition as the singular behavior near $x = 0$ is very sensitive to the unknown value of μ_0 —the effective value of γ is a rapidly varying function of μ_0 [25]. Since QCD evolution due to parton radiation is mainly responsible for the rise of the parton density at small values of x , it is also natural to assume logarithmic factors of the form $\log^\delta(1/x)$ at a given μ_0 . The variation of the parameters γ and δ with μ_0 and the range of values of these parameters consistent with current experiments have been systematically studied in [25]. The parametrization of the small- x behavior of parton distributions in the context of global analysis of data will be discussed in Sec. 5.4 and Sec. 7.

4 Reference Processes

4.1 Deep Inelastic Scattering

Deep inelastic lepton-nucleon scattering provided the first evidence in support of the original parton model. Since then, this process has played a leading role in the determination of parton distributions because it probes the structure of the target hadron via the clean and well understood weak or electromagnetic current. In the LO QCD parton model, the “hard cross sections” reduce to just electroweak coupling constants multiplied by an on-shell delta function which removes the convolution integral, so the physically measurable deep inelastic scattering structure functions become simple linear combinations of the parton distribution functions $f_A^q(x, \mu)$. For example, the structure function F_2 measured in eN or μN scattering has the form

$$F_2^N(x, Q) = x \sum_q e_q^2 f_N^q(x, Q) \quad (\text{leading order}) \quad (12)$$

where e_q denotes the charge of the quark q . The factorization scale μ has been identified with the characteristic momentum scale Q (virtual mass of the exchanged vector boson) of this hard scattering process.

The complete set of relationships for all measurable structure functions can be found in [26]. This kind of direct relationship has led to the wide-spread practice of referring to the parton distribution functions $f_A^q(x, \mu)$ also as “structure functions”, which in turn has fostered the tantalizing misconception among many that parton distribution functions are “physical” (*i.e.*, directly measurable) objects. Unfortunately, the simple connection between the two quite distinct concepts holds only in leading order. Indiscriminant mingling of the two can lead to incorrect conclusions. As emphasized throughout this review, for quantitative applications of the QCD parton formalism, it is crucial to recognize the “unphysical” aspects of the parton distributions (*i.e.*, renormalization scheme- and scale-dependence) as well as their attractive physical interpretations.

In LO order, the gluon distribution affects the measurable structure functions only via the quark evolution equation, Eq. (6); one must go to higher orders in order to probe the gluon distribution directly. In NLO, one has

$$F_2^N(x, Q) = x \sum_q e_q^2 f_N^q(x, Q) + \alpha_s(Q) \left[\sum_q C_2^q \otimes f_N^q + C_2^g \otimes f_N^g \right] \quad (13)$$

where the symbol \otimes indicates a convolution. The coefficient functions $\{C_2\}_{\overline{MS}}$ were calculated early in the development of QCD using the \overline{MS} subtraction scheme [27, 28]. The explicit appearance of the gluon distribution on the right-hand-side of this equation, however, does not necessarily give a good handle on f_N^g . First, this term is small compared to the leading quark term; more importantly, it is possible to exploit the arbitrariness of choice of factorization scheme to *define away* the entire NLO term in Eq. (13) (arising from the hard scattering part in the \overline{MS} -scheme) by absorbing it into the LO quark term with a new definition of the quark distribution functions (the soft part of the factorization theorem) [28]. In the new scheme – often referred to as the DIS-scheme – the NLO formula for F_2^N is, by definition, the same as the LO one (Eq. (12)), i.e. $C_{2DIS}^q \equiv C_{2DIS}^g \equiv 0$, hence there is no apparent gluon dependence. (We will discuss the issues on choice of scheme below and in Sec. 5.3 and Sec. 7.)

The gluon distribution does, however, contribute directly to the observable longitudinal structure function $F_L(x, Q)$ and to the rate of change of the structure function $F_2(x, Q)$ with respect to Q . Both are intrinsically order α_s effects. Specifically, we have:

$$F_L^N(x, Q) = \alpha_s(Q) \left[\sum_q C_L^q \otimes f_N^q + C_L^g \otimes f_N^g \right] \quad (14)$$

where the coefficient functions C_L are well-known [27]–[29]. The simplicity of this equation makes this potentially the best means of measuring the gluon distribution, especially because the dominant part of the quark term can be related to the measurable $F_2^N(x, Q)$, cf. Eq. (12) [30].

The rate of change of the structure function $F_2(x, Q)$ with respect to Q , is given by

$$\frac{dF_2^N(x, Q)}{dt} = \int_x^1 \frac{dy}{y} \left[P_{qq}(y) F_2^N\left(\frac{x}{y}, Q\right) + \left(\sum_q e_q^2 \right) P_{qg}(y) f_N^g\left(\frac{x}{y}, Q\right) \right] \quad (15)$$

where $t = \ln Q^2/\Lambda^2$. Eq. (15) is obtained from the first of the evolution equations Eq. (6) by multiplying with $x e_q^2$, and summing over q . Since $F_2(x, Q)$ is the most accurately measured structure function, this relation offers a useful method to constrain the gluon distribution, at least in the region of small x values where the gluon term in Eq. (15) makes a significant contribution.

In LO, the structure functions, F_i ($i = 1, 2, 3$) measured in νN or $\bar{\nu} N$ scattering depend on different linear combinations of parton distributions [26]. With sufficiently

precise data over a wide enough kinematic region, one can separate the valence and sea quark distributions. However, the various flavors of sea quarks cannot yet be readily differentiated due to the fact that: (i) quarks of different generations contribute to the measured quantities in the same way, and (ii) current experimental practice is to combine the ν and $\bar{\nu}$ measurements (to increase statistics), rather than to use them separately to yield independent linear combinations of parton flavors. This issue will be discussed in Sec. 7.

In NLO, both structure functions F_L and F_3 acquire non-trivial order α_s corrections, similar to Eq. (13). This is true even in the DIS scheme which is designed to make F_2 simple, as described above. Since F_2 has no particular significance in theory, the DIS scheme does not have any special status except a historical one. This is becoming clearer as the application of the QCD formalism expands to an ever increasing number of physical processes beyond deep inelastic scattering.

Because at least two different schemes are commonly used in the current literature, and because this has been a continuing source of confusion (and hence misuse of the QCD parton model, *cf.*, Sec. 5.3 and Sec. 7), it is useful to review the definition of these schemes and specify the relation between them. The $\overline{\text{MS}}$ -scheme is defined by a universal prescription to calculate perturbative matrix elements independent of any physical process [27]. The $\overline{\text{MS}}$ -scheme parton distributions are those which appear in equations such as Eq. (13) and Eq. (14) with the hard-scattering part (C_i) calculated with the $\overline{\text{MS}}$ subtraction prescription. It can be shown that the quark number sum rules and the momentum sum rule are automatically satisfied in this scheme. On the other hand, the DIS scheme, as described above, is specially designed to render the simple parton model deep inelastic scattering structure function formula Eq. (12) for F_2 applicable even at NLO. Comparing the NLO equations for F_2 in the two schemes, it is easy to determine the transformation formula for quark distributions defined in these two schemes:

$$f_{DIS}^q = (1 + \alpha_s(Q)C_{2\overline{\text{MS}}}^q) \otimes f_{\overline{\text{MS}}}^q + \alpha_s(Q)C_{2\overline{\text{MS}}}^q \otimes f_{\overline{\text{MS}}}^q/2n_f^{eff}. \quad (16)$$

Within the context of deep inelastic scattering, there is no obvious counterpart to Eq. (16) for the gluon, since it does not couple directly to the electroweak current. Among possible choices to specify the gluon distribution in this scheme, the natural requirement that the momentum sum rule be preserved (in order to maintain the parton model interpretation) motivates the definition:

$$f_{DIS}^g = (1 - \alpha_s(Q)C_{2\overline{\text{MS}}}^g) \otimes f_{\overline{\text{MS}}}^g - \alpha_s(Q) \sum_q C_{2\overline{\text{MS}}}^q \otimes f_{\overline{\text{MS}}}^q. \quad (17)$$

which is adopted by most groups working with the DIS scheme. Because this latter equation is not unique, it is prudent to ascertain the precise definition of the gluon when a given set of DIS distributions is used.

As perturbative formulas, Eq. (16) and Eq. (17) can easily be inverted (to $O(\alpha_s)$) in order to derive $\overline{\text{MS}}$ distributions from a given set of DIS distributions. This is safe as long as the NLO terms remain small compared to the leading term. Two cases in which this condition is not met has been noted in [7] and they will be discussed in Sec. 7.

4.2 W, Z, and Lepton-pair Production

The production of W and Z bosons, as well as massive lepton pairs (via time-like virtual vector bosons), in hadron collisions is related to one-particle production in deep inelastic scattering by crossing one lepton and one hadron line. We shall refer to these processes generically as vector boson production and use γ^* as the representative example except when otherwise noted.

The lowest order process in this case is the Drell-Yan [31] process $q\bar{q} \rightarrow \gamma^*$. As in the deep inelastic case, gluons contribute in the next order through the elementary processes $gq \rightarrow \gamma^*q$ and $q\bar{q} \rightarrow \gamma^*g$. Results on the Q^2 and y (or x_F) distributions can be found in [32] and [33]. The ratio of the full $O(\alpha_s)$ result to that of the lowest order, the so-called “K-factor”, was found to be unexpectedly large – about two. This was largely due to two effects: (i) the continuation of the vector boson mass Q from space-like values in deep inelastic scattering (where the conventional parton distributions were defined) to time-like values for vector boson production introduces a factor of π^2 in the correction term; (ii) the phase space boundaries for the two processes are different, which generates some additional large corrections near the kinematic boundary.

The large corrections raised questions about the reliability of perturbative calculations and inspired in-depth studies of the nature of these corrections and the means to control them. Much work has been directed toward calculating the next higher order terms to gain more information on the corrections. Recently, the full second order calculation has been completed – see [34] and references therein. An alternative approach is to identify the origin of the large corrections and then to use this knowledge to resum the perturbation series, thereby taking into account this type of correction to all orders. Steady progress has also been made along this line [35]. The two approaches are complementary; it has been shown that the resummed result (which exponentiates) reproduces the bulk of the next higher order results over most of the kinematic region—a very encouraging indication that the large corrections can be “understood” and quantitatively controlled [35]. Further advances can be made in simplifying the resummed results and in expanding the kinematic regions where similar techniques can be applied.

Because the exponentiated correction factor has certain universal properties among hadron-hadron processes, Sterman has suggested that it may be desirable to absorb this factor into the definition of parton distributions when analyzing hadron processes [36]. The “advantage” would be that the remaining hard scattering part would contain only intrinsic higher order effects. This proposal would result in two classes of parton distributions – one for lepton-hadron and one for hadron-hadron – which would be related by known factors. Whether the proposal is adopted in practice or not, it is only a matter of convention which does not affect the underlying physics if used consistently, just like the scheme dependence discussed before.

In addition to the integrated cross section and the rapidity distribution, perturbative QCD has also been applied to study the p_T distributions of vector boson production. This requires more sophisticated resummation methods because the presence of more than one large scale (say, Q and p_T) which give rise to additional large

logarithms in regions where their ratio is large. The theory has been well-established [37, 38]. The first calculation of the W-vector boson p_T distribution yielded a qualitative description of measurements at the hadron colliders. A recent NLO perturbative calculation of the vector boson p_T distribution has been shown to merge well into the resummed formula obtained earlier [39]. Detailed phenomenological work on the analysis of vector boson p_T distribution, especially in the context of providing information on parton distributions has not yet been done.

4.3 Direct Photon Production

The production of photons with large transverse momentum in hadron-hadron collisions is known to be sensitive to the gluon distribution. The two Born processes, both of $O(\alpha_s)$, are $q\bar{q} \rightarrow \gamma g$ and $gq \rightarrow \gamma q$. In pp interactions the contribution from the $q\bar{q}$ subprocess is small, leaving as the dominant term one which is directly proportional to the gluon distribution. An $O(\alpha_s^2)$ calculation of the invariant cross section has been performed [40] and a program for calculating the cross-section based on this work is widely available. The theory appears to be in good agreement with the data currently available. Reviews can be found in [6, 41, 42]. Recently, a higher order calculation of the photon-plus jet cross section has been performed [43, 44] which also agrees with the available data [45].

Photons, whether real or virtual, or appearing in the initial or final state, are good probes of hard scattering processes to the extent that they participate directly in the hard scattering process. However, in the case of photon production, this apparent advantage is diminished by some complications. Specifically, direct photons are not *a priori* distinguishable from radiative photons (*i.e.*, bremsstrahlung) accompanying high- p_T partons produced in regular hadron hard scattering. Such photons will, however, tend to be produced nearly collinear with the parent parton. Indeed, one can define photon fragmentation functions [46] which satisfy a set of evolution equations modified by the addition of an inhomogeneous term. The leading-logarithm contribution to the solution is independent of input boundary conditions and simple parametrizations of these are available [6]. The contributions of such terms to the fully inclusive cross section are generally significant only in the small x_T region, so that determinations of the gluon distribution in the mid- to large- x range are not affected to any large degree. However, in collider experiments it is often necessary to place rather restrictive isolation cuts on the electromagnetic triggers in order to obtain a relatively clean sample of direct photons. That is, it is necessary to limit the amount of hadronic energy in the vicinity of the photon. This cut removes a portion of the bremsstrahlung signal, but not all of it. Theoretically, this might seem to render the isolated cross section incalculable (because it is, strictly speaking, not infra-red safe), but such is not necessarily the case as is discussed in [47]. It is shown that the isolated photon cross section can be calculated perturbatively as long as the cuts are not too restrictive.

The higher order calculation described in [43] can take these isolation cuts into account – the integrations are done using a combination of analytic and Monte Carlo methods in order to maximize the flexibility of the program with regard to calcu-

lating different observables. While this is very useful for generating various types of predictions to be compared with experiment, it is not adequate for incorporation into a large fitting routine because of the time required to generate accurate answers and the statistical errors associated with Monte Carlo integration. A new program for the isolated cross section is being developed which does not utilize Monte Carlo methods [48].

4.4 Heavy Quark Production

The production of heavy quarks in lepton-hadron and hadron-hadron collisions provides good tests of QCD. In this case the heavy quark mass sets the large scale needed to justify the use of perturbative techniques. Charm production in charged current lepton-hadron scattering experiments has been the main source of information on the strange quark distribution inside the nucleon. Similarly, its production in neutral current scattering can determine the charm content of the nucleon. At the higher energies of ep colliders, bottom and top quark production may also become available. Heavy flavor production in high energy hadron collisions is sensitive to the small- x behavior of gluons and quarks.

The LO calculation of heavy quark production in lepton-hadron scattering appears to be straightforward. The effect of the heavy quark mass has been incorporated in all existing phenomenological applications in the form of “slow- rescaling” reflecting the modified on-shell condition for the heavy quark (*cf.* [26] for a review). But, interestingly enough, none of the existing applications, both theoretical and experimental, even use the full LO hard matrix element and the complete kinematics appropriate for heavy quark production which can have equally important effects on the analysis. In addition to the need for correcting these deficiencies, it has been pointed out recently that, the mixing of heavy quarks with gluons and the abundance of gluons inside the nucleon require at least the NLO formulation of this process in order to be meaningful [7, 49]. NLO calculation of the hard cross-section for this process have been calculated recently by several groups [49]–[51]. The implementation of the QCD formalism, even with known NLO hard cross-section, is tricky in the region not far above the heavy quark threshold where most experimental data lie. The method for calculating heavy particle production developed in [52], which is used in [49], ensures physically meaningful results from the threshold to the asymptotic regime.

Heavy flavor production in hadron collisions has, so far, not played any role in parton distribution analysis, due to the experimental difficulty in measuring the relevant cross-sections. Theoretical calculations on the hard cross-sections have been carried out to order α_s^3 by two different groups.[53, 54]

4.5 Other High- p_T Processes

Progress continues to be made on higher order calculations for various types of hard scattering processes. These types of calculations are important for a variety of reasons such as performing more precise tests of the standard model and obtaining better estimates of standard model backgrounds to signals of new physics. Most notable among

purely hadronic processes is the $O(\alpha_s^3)$ calculations of the single jet invariant cross section [55, 56]. Phenomenological applications of these calculations can place some constraints on parton distributions or discriminate between existing distributions, especially for the gluon which gives the dominant contribution to hadron scattering at high energies.

Another area of QCD applications where much progress has been made is multi-jet and $W + \text{jets}$ production – both at tree level [57] and, recently, at the 1-loop level [58]. In order to gain control of these complicated calculations, many new techniques on powerful helicity amplitude analyses, color factor algorithms, and (4-dimensional) superstring technology have been developed and brought to bear [59]. At present, these calculations can help in understanding the observed experimental features. However, the phenomenology is still quite far away from being able to quantitatively give feedback on the parton distributions.

5 Global Analyses

Ideally, the global analysis of parton distributions involves making use of experimental data from a complete set of physical processes in a QCD analysis to extract a unique set of universal parton distribution functions. These can then be used in other applications, *e.g.*, to make predictions for other conventional processes, to provide stringent tests of the self-consistency of the perturbative QCD framework itself or of the Standard Model in general, and to search for new physics. We review the progress which has been made toward achieving this goal. We discuss recent experimental developments and relevant experimental, theoretical, and phenomenological issues and uncertainties involved in such analyses. For this purpose, it is helpful to have a global view of the physical processes contributing to parton distribution analysis, particularly the relevant kinematic ranges covered by the various types of experiments. A “map” for such a global view was compiled at the Snowmass 90 Workshop [60].

5.1 General Strategies and Review of Recent Developments

Deep inelastic scattering of leptons on nucleon and nucleus targets remains the primary source of information on parton distributions. For a review of the experimental results up to 1989, see [61]. The original high-statistics, high-energy data of the early 1980’s, on which the first generation of parton distributions were based, have been superseded in the last few years by much more accurate data from recent muon-scattering (BCDMS[62]) and neutrino-scattering (CHARM[63], CDHSW[64], FMM[65] and CCFR[66]) experiments. The substantial changes in experimental data (up to 15-20% in some regions such as small- x) necessarily make the pioneering parton distribution sets obsolete for modern applications. Significant recent developments on the experimental front are:

(i) the emergence of very accurate new and re-analyzed SLAC-MIT electron-scattering data [67] as well as the re-analyzed EMC data [68] has finally resolved the much publicized BCDMS - EMC controversy [69];

(ii) the unveiling of new Tevatron neutrino data [66] [65], especially those of CCFR, revealed impressive general agreement with QCD expectations (much like the earlier results of BCDMS for muon data);

(iii) new NMC results [70] yield fresh information on differences in the neutron and proton structure functions and expand the measured kinematic range to ever smaller values of x .

Recently a comprehensive and easily accessible database on deep inelastic scattering structure functions has been compiled by the Durham-RAL group [71]. This greatly facilitates future phenomenological work on deep inelastic scattering and on global analysis in general. As clearly shown in [71], deep inelastic scattering data are in very good shape as the foundation for parton distribution analysis. In addition, major advances are eagerly awaited when HERA comes on-line.

However, as is well-known, the inclusive DIS structure functions are mostly sensitive to certain combinations of quark distributions. Hence even the most accurate DIS data do not place tight constraints on the gluon distribution at intermediate or large values of x and they are not effective in differentiating all the quark parton flavors.

Vector boson production – including the production of lepton-pairs, direct photons at large transverse momenta, and W 's and Z 's – provides important complementary information on parton distributions. Lepton-pair production has several unique features: (i) cross-sections in pN collisions are directly proportional to the anti-quark distributions; (ii) cross-sections in πp (and $K p$) collisions offer one of the few handles on parton distribution functions in mesons; (iii) the measured A -dependence provides complementary information on the “EMC-effect” [72]. The relatively new Fermilab E605 results [73] provide a significant improvement over earlier fixed-target experiments, both in accuracy and in kinematic coverage. Combined analysis of these data with DIS leads to much more tightly constrained parton distributions than those obtained with DIS data alone [74]. Collider results for this process will offer a significant opportunity to probe the small- x region (say, $x \leq 10^{-3}$, see Sec. 7).

Direct photon production is particularly sensitive to the gluon distribution and, therefore, can play an important role in global analyses (see Sec. 4.3). The measurement of the angular distribution of the photon compared to that for π^0 's in the parton-parton center of mass frame shows the flatter distribution expected from theory, confirming the presence of direct photons. Combining direct photon and deep inelastic data together in a simultaneous analysis places much stronger constraints on the gluon distribution than using deep inelastic scattering data alone, as was shown in [75]. This analysis used data for the invariant cross section from the WA-70 experiment [76] at 280 GeV/c. The data were sensitive to the gluon distribution in the region of x from 0.35 to 0.55, thereby complementing the information available from deep inelastic scattering which is sensitive to the gluon distribution at smaller values of x . The data available so far will be greatly enhanced by anticipated results from the Fermilab experiment E706 [77].

Collider experiments on direct photon production probe gluons at a smaller x region. Complications due to bremsstrahlung contributions and photon isolation cuts have been brought under better control. (See Sec. 4.3). New programs are being developed which will make it possible to include collider data into the global analysis. Data from CDF and D0 in the near future will undoubtedly contribute to the determination of the gluon distribution.

In principle, additional sensitivity to the gluon distribution can be obtained by using data for the photon plus jet cross section. Knowledge of the four-vectors of both the jet and the photon allows the underlying parton kinematics to be more tightly constrained. This reduces the amount that the parton distributions are smeared out by the convolutions in going from the parton level to the observed particles. Furthermore, the useful range in x where the data can be used to constrain the gluon distribution can be extended if sufficient rapidity coverage is available. To date, such data have been provided only by one experiment [45] and both the photon and jet were constrained to be centered on $y = 0$. However, several other experiments expect to have new data for this observable in the near future. The benefits which result from more precise knowledge of the hard scattering kinematics are gained at the expense of limiting statistics since the data set will be distributed over more bins. It remains to be seen whether sufficient statistics can be obtained to usefully constrain the fitting process.

Finally, W and Z production in colliders, especially from the increasingly accurate measurements at the Tevatron, provides additional information on the parton structure of the proton [78]. So far, only existing distributions have been used to interpret the measured results. However, with increasingly abundant and accurate data on the W-asymmetry, W/Z ratios, etc., one will be able to determine some important aspects of parton distributions (such as the u/d ratio) from these data. Since the Q^2 value for these data is enormous compared to other processes, the relative contribution due to the charm quark is large, making this a potential source of information for the charm distribution [79].

5.2 Experimental Considerations and Uncertainties

Due to greatly improved experiments, current global analyses must take into account many details which were usually left out of earlier efforts. A discussion of relevant issues has been provided by the *Structure Functions and Parton Distributions* group in the 1988 Snowmass Workshop [26]. We shall summarize the key points and refer the reader to Refs. [26] and [3] for details.

In most modern high statistics experiments, the experimental errors are now predominantly systematic rather than statistical. Understanding these errors is a major part of these experiments, and often takes years of effort. Thus it is important to incorporate the systematic errors in the phenomenological analysis. Since systematic errors are usually correlated, this is much harder to do than the common practice of including only the point-to-point statistical errors. Often times, this cannot be done properly without close cooperation between experimentalists and theorists.

In a global analysis using data sets from a wide range of experiments, additional

caution is needed. First, even among experiments of the same type, different groups often apply quite different theoretically motivated “corrections” to the (experimentally corrected) data in arriving at the final results on a given physical quantity. In deep inelastic scattering structure function measurements, for example, common corrections include: longitudinal structure function (QCD, experiment, or 0), “strange sea”, “isoscalar”, and “slow rescaling”. The discrepancies resulting from varied practices in applying these corrections can be quite significant [26] and have sometimes been found responsible for troubling controversies. (For instance, a part of the well-known BCDMS-EMC controversy at low values of x is now attributed to the fact that EMC assumed a vanishing longitudinal structure function while BCDMS used the QCD prediction [68]). Clearly a valid phenomenological analysis must pay close attention to all potential sources of discrepancies of this type.

Global analyses usually are based on least chi-square or maximum likelihood methods. When combining several different types of processes, involving experiments with a wide range of statistical and systematic errors, the proper definition of overall chi-square and/or likelihood is not obvious. To obtain precise determinations of the QCD parameters and parton distributions requires careful thought and a great deal of systematic phenomenological study. Efforts along this line are only beginning.

5.3 Theoretical Considerations and Uncertainties

The perturbative QCD approach has certain inherent limitations and uncertainties which need attention in any systematic study. Some of these limitations can be overcome by further theoretical developments, and hence represent current frontiers in QCD research. All have to be clearly recognized, and included in the assessment of uncertainties in state-of-the-art global analyses.

Factorization Scheme: When performing next-to-leading order global analyses close attention must be paid to the consistent choice of the factorization scheme used in defining the parton distributions and the hard cross-sections in *all* processes, as emphasized in Sec. 2.2. Two schemes — the “DIS” and the “ $\overline{\text{MS}}$ ” schemes — are widely used in the literature. In principle, parton distribution functions obtained in one scheme can be readily transformed into the other scheme. However, the transformation is not unique, as discussed in Sec. 4.1. Comparison of these two schemes and cautions on their proper use will be discussed in Sec. 6.

Renormalization and factorization scale dependences: The truncation of the perturbation series invariably leads to renormalization and factorization scale dependence of QCD predictions, as discussed in Sec. 2.2. However, in almost all processes where beyond leading order results are known, one can clearly see a decrease in the dependence of the predictions on the choice of scale as higher order terms are included. This underlines the importance of carrying out calculations to adequately higher orders. Unfortunately, the sensitivity to the choice of scale varies from process to process. Thus, in practice, the uncertainty associated with the choice of scale can only be assessed phenomenologically by varying the relevant scales over reasonable ranges. If significant scale dependence is found to exist in a particular kinematic region for some process, then the usefulness of such data will be reduced until new theoretical

techniques are developed to reduce that dependence. (See below.)

Higher order corrections: The uncertainty associated with higher order corrections beyond current calculations (see Sec. 4) cannot be reliably estimated in general. One manifestation of this uncertainty is the scale dependence described above. That is, however, not the whole story. In special kinematic regions, relatively large corrections can be identified on physical grounds. Often times, the bulk of these effects can be calculated by special resummation techniques. Prominent examples are: the small- x region, the threshold region (x near 1), and the small transverse momentum region (*cf.* Sec. 4.2). Advances in these fields help to reduce the uncertainties and improve the reliability of the phenomenological analyses. Implementation of the higher-order (or “all-order”) corrections, however, inevitably makes such calculations quite complicated and more removed from the simple intuitive parton model results.

Higher-twist effects: Contributions to hard scattering cross sections which are suppressed by powers of the relevant large momentum transfer are referred to as “higher-twist” corrections. These become insignificant at very high energies in regions far from the kinematic boundaries, but may not be entirely negligible at moderate energy scales where a great deal of current data exist. The theory for power-law terms is known to be much more complicated than the leading twist one [80]. Nevertheless, factorization properties for the twist-4 corrections to conventional perturbative QCD have recently been established [81]. The first foundation for phenomenological work in the relatively low Q^2 region appears to be laid. Recent convergence of the wide-range of high-precision DIS data, spanning the entire range of Q^2 from 1 to 300 GeV², described earlier, sets the stage for detailed QCD analyses incorporating higher-twist components. The emerging new results from NMC and E665 will complement existing data, especially in the small- x region, in a comprehensive phenomenological study. Since there are many more theoretical unknowns than in the standard twist-two formalism, realistic applications must invoke certain phenomenological ingredients in addition to the established theory. If this proves fruitful, it will help improve the conventional twist-2 QCD parton analysis by providing a smooth transition into the low Q^2 range without an arbitrary kinematic cut (see below). An interesting example of this can be found in the analysis presented in [82].

5.4 Phenomenological Considerations and Uncertainties

Kinematic cuts: The outcome of a given global analysis depends on the selection of physical processes as well as on the experimental kinematic range of data. To ensure the applicability of the conventional perturbative QCD formalism, it is desirable to make reasonably high cuts in dimensional variables such as Q, W . On the other hand, experimental data are usually much more abundant in the low Q region; and, in addition, it is much easier to get an handle on the predicted logarithmic QCD scale-dependence at moderate values of Q (as it diminishes at high energies). Thus, it is important to consider the optimal choice of kinematic cuts in data selection and to determine the dependence of the results on this choice [74, 83]. As noted in [82], the inclusion of target mass corrections and phenomenological higher twist terms can extend the useful Q range to smaller values than would otherwise be the case.

Nuclear target effects: Our primary concern is the parton structure of the nucleon. However, many of the key fixed-target experiments in deep inelastic scattering and lepton-pair production use nuclear targets. The so-called “EMC-effect” [84] demonstrates that nuclear structure functions are not simple incoherent sums of the corresponding nucleon ones — the ratio shows a distinct x -dependence, deviating from unity by up to 10–15%. Theoretical understanding of this phenomenon is not complete, and lacks predictive power over the full x -range. In practice, corrections are usually made on a phenomenological basis by using experimentally measured ratios whenever possible. Whereas this procedure should be quite reliable when applied to the same physical process, the uncertainty of using correction factors measured with one probe (muon) on another (neutrino) is not known *a priori*.

Normalizations, shapes, and ratios: Under certain situations, theoretical uncertainties in the determination of parton distributions can be reduced by focusing on specific aspects of measured cross-sections such as the shape of some differential cross-sections, ratios of cross-sections, and asymmetries. For example, it has been shown that the shape of the direct photon p_T distribution is sensitive to the gluon distribution, whereas the normalization is more dependent on the value of the coupling constant [75]. Since experimental normalization uncertainties are usually hard to pin down in the first place, it then makes sense to allow an overall floating normalization factor for some or all experiments in the global analysis. Note that the overall normalization of the parton distribution functions are constrained by the quark number and momentum sum rules. Of course, within one experiment, measured cross-section ratios and asymmetries always have much less associated uncertainty, and thus can be used with advantage whenever appropriate. For instance, the forward-backward asymmetry in W production and the W -to- Z production ratio at the hadron colliders, when they are more accurately determined, are expected to yield valuable information on the u/d ratio and the charm content of the nucleon.

Effects from the choice of parametrization of the initial distributions: There is considerable freedom in choosing the parametric form of the initial parton distributions (at scale Q_0) in making the global analysis. The parametrization must be general enough to accommodate all the possible x and quark-flavor dependences; but it should not contain so many parameters that the fitting procedure becomes very much under-determined [74, 83]. In practice, most groups use a functional form

$$f^a(x, Q_0) = A_0^a x^{A_1^a} (1-x)^{A_2^a} P^a(x) \quad (18)$$

where a is the flavor label (including the gluon), and $P^a(x)$ is a smooth function. The choice of $P^a(x)$ varies considerably — examples include polynomials in x of various degrees or logarithmic forms such as $\log^{A_3^a}(1/x + 1)$ [74]. To reduce the large number of parameters to a more practical size, various simplifications are usually made (such as setting the A_i^a 's to specific values and assuming flavor independence of various coefficients), based on educated guesses. The question is: how are the final results dependent on these assumptions?

It is very difficult to quantify the uncertainties resulting from the choice of parameters and the functional form for $P_a(x)$, although it is obvious that inappropriate

choices can bring about misleading results. The small- x behavior of the parton distributions and the flavor dependence of the sea-quark distributions at a general scale Q are strongly dependent on the assumptions made about the relevant parameters for the initial distributions at Q_0 . The only definitive way to resolve these uncertainties is to compare theory with experiment in processes which are sensitive to these parameters. This requires persistent work which is updated constantly with advances in both theory and experiment. Where uncertainties are present, it is very important to systematically study the limits on the relevant parameters set by existing theory and experiment. Work in this direction is only beginning [85].

One attempt to reduce the dependence upon ad hoc parametric forms is to generate as much as possible of the parton distributions via the evolution equations themselves. Such distributions are generally referred to as radiatively generated parton distributions, a recent example of which can be found in [86]. The basic idea is to use a minimal set of input parton distributions (say, only valence quarks with or without gluons) at a relatively small scale Q_0 , typically in the range of $2\Lambda - 3\Lambda$. The bulk of the sea and gluon distributions will then be arrived at by evolution, driven primarily by the valence terms. A review of this approach can be found in [87].

5.5 Parametrizations of Results

The results on parton distributions from a global analysis can be presented in two ways. First, if the parametrization of the initial distributions and all the QCD parameters are given, any user can accurately recreate the distributions at all (x, Q) by using a QCD-evolution program with these as input. This is not usually done. Instead, the common practice is to approximate the outcome of a global fit over all (x, Q) by a set of parametrized functions. The way this approximation is made varies widely between the available distribution sets, ranging from a simple interpolation formula over a large three-dimensional array (x, Q , and flavor), to Chebeshev polynomial expansions of the functions, to simple Q -dependent parametrizations of the form of Eq. (18).

Although, in principle, the form of the approximation is transparent to the user of the distributions, there are circumstances under which misleading results can arise from a lack of understanding of the parametrization. For instance, in applications to very high energy processes, the convolution integral in the QCD parton formula Eq. (2) often involves extremely small values of x — beyond the range where the parton distributions were originally derived — resulting in inadvertent extrapolations of the distributions. This can lead to quite unrealistic results if the functions behave badly beyond the originally intended range (*e.g.*, negative, oscillatory or discontinuous — examples of all these cases happen for some existing distribution sets). The danger is that the user won't even know that the results are unreliable, unless they are obviously absurd. This problem is eschewed with a parametrization using positive-definite functions smooth in both variables (x, Q) , such as done in [74] with $P^a(x, Q) = \log^{A_f^a(Q)}(1/x + 1)$ in Eq. (18). (See also [74, 25] for a detailed discussion of the other advantages of this parametrization).

6 Survey of Recent Parton Distributions

The first generation parton distribution sets, based on leading order evolution and data of the early 1980's, have been widely used for calculation of high energy processes [88]. However, experimental data have drastically improved (and substantially changed, in some cases) since then, and most current applications require at least next-to-leading (NLO) order treatment. Therefore, second generation global analyses based on NLO evolution and more current data have been made by several groups in recent years. Broadly speaking, these can be categorized into two groups: (i) specialized analyses focusing on some specific issue or process (such as the gluon distribution and direct photon production [75], neutrino scattering [89], and radiatively-generated parton distributions[86]); and (ii) global analyses encompassing a wide range of processes [74, 90, 91, 92]. These analyses differ considerably in many aspects on issues discussed in the previous section, *e.g.* the range of data used, the way experimental errors are treated, the choice of renormalization scheme, and assumptions on the initial distributions, etc. Consequently, a critical comparison of these distribution sets is quite difficult, if not impossible.

A compilation of currently available parton distribution sets, both old and new, has been made at CERN and it has been recently distributed as a program package PDFLIB[93]. We refer the reader to this package for detailed references and some comparison plots. It is important to note however, that the very convenience resulting from having all published distributions at once also tends to encourage indiscriminant use of these distributions in the hands of inexperienced users, given the complexity of issues discussed before. We shall highlight some of the most relevant considerations in putting these distributions in perspective.

In evaluating different sets of parton distributions or calculations of some physical quantity based on these distributions, it is essential that meaningful corresponding objects are compared. On the parton distribution level, LO, NLO- $\overline{\text{MS}}$, and NLO-DIS distributions, like apples and oranges, should not be compared with one another — as is often done, *e.g.*, even in the PDFLIB document [93]. To illustrate this point, we show in Figure 2a two curves each from the MT-S2 and HMRSB parton distribution sets corresponding to the *same* strange quark defined in the DIS and $\overline{\text{MS}}$ schemes respectively. The transformation between the two functions is performed according to Eq. (16). The significant difference between the two functions, especially in the small- x region, arises from the large contribution of the gluon term on the right-hand-side of the equation, reflecting the quark-gluon mixing effect in changing from one scheme to the other. Since the gluon distribution is numerically one order of magnitude larger than the sea quark, the nominal order α_s term can be quite significant compared to the “leading” term. The actual size of the effect depends very much on the specific input distributions. Examples where the effect is even larger than shown in Figure 2a can easily be found [49]. Likewise, in Fig 2b we show the same comparison for the gluon distribution. Note the big difference, in the large- x region, between the curves for the *same* distribution in two different schemes (MT-S2(DIS) & MT-S2($\overline{\text{MS}}$)) — in contrast to the relatively small difference between the results from the two entirely independent analyses expressed in the same scheme (HMRS-B & MT-S2($\overline{\text{MS}}$)). In this

case, the large difference arises from mixing of the gluon with the much larger valence quarks in the large- x region [74]. These results demonstrate that at moderate values of Q , it is almost meaningless to talk about a LO sea-quark or gluon distribution; only at the NLO level do these quantities acquire unambiguous meaning, provided the choice of renormalization scheme is specified. In this regard, the situation is rather like the case for the QCD coupling α_s , as discussed in Sec. 2.3.

On the level of physical quantities, LO, DIS, and $\overline{\text{MS}}$ distributions must be convoluted with the corresponding LO, NLO-DIS, and NLO- $\overline{\text{MS}}$ hard scattering cross section formulas in order to yield meaningful predictions, as emphasized in earlier sections of this review. Applying parton distributions defined in different schemes to the same hard scattering cross section formula to make comparisons, a practice too often seen in the literature and conference reports up to now, is simply meaningless and distracts from real physics issues.

It should be self-evident that, for use in quantitative applications of QCD, the first prerequisite which the parton distributions should satisfy is that they fit the well-established data. Paradoxically, this obvious point has been consistently ignored in the eagerness to present results with either a favorite distribution set, or with a variety of distribution sets in order to show the supposed range of “theoretical uncertainties” — even if these are already known to disagree with current data. It is worthwhile to point out in this regard that, contrary to general impressions, even the recent second generation distribution sets do not necessarily fit existing high-precision data. In Figure 3 we show a representative comparison of BCDMS data with predictions from three commonly used NLO distribution sets. The significant departure of the prediction of the widely used DFLM distributions from data is due to the fact that muon-scattering data were not used in the analysis for their extraction.

There are contemporary applications of QCD, such as certain estimates for LHC and SSC physics, which do not require NLO accuracy or for which the required NLO calculations have not been performed. The LO formalism is attractive because the numerical calculation is generally at least one order of magnitude faster than the NLO one. Obviously, even in LO calculations, it is desirable to use parton distributions which agree with current data. It is for this purpose, two recent LO parton distribution sets have been published [74, 94].

7 Current Uncertainties and Immediate Challenges

In principle, given a complete set of experiments, one can determine all the independent parton distributions using the QCD formalism. In practice, due to existing limitations of both theory and experiment, the program of a comprehensive global analysis of parton distributions is still in an evolving state. In this section, we discuss how to assess uncertainties on parton distributions, identify the main areas of current uncertainty, and spell out the challenges involved in overcoming them.

A seemingly simple way to exhibit the uncertainty on parton distributions is to plot or tabulate a large number of published distribution sets side-by-side and expose

the range of differences. An inspection of a typical such plot, *e.g.*, in [93], will show a rather wide range of variation for all the parton flavors — in apparent sharp contrast to the extreme accuracy of current experimental data on DIS structure functions from which these distributions are extracted.[71] Such comparisons are, of course, totally misleading for reasons already discussed in the previous two sections. A better way, along the same line, is to make the comparison using only distribution sets defined in the same scheme, to the same order, and which all fit the relevant current data. Figure 3 and Figure 4, discussed below, are sensible comparisons of this kind. One will see that the spread between currently viable distributions of the same type is *much less* than what is commonly perceived.

However, even this procedure does not necessarily reveal the true range of uncertainty because different published distribution sets may invoke different assumptions and use different short-cuts in dealing with the experimental and theoretical issues in their analysis (see Sec. 5). In addition, in all global analyses, there is a certain arbitrariness in selecting the final distributions (for publishing or circulation) from a fairly wide range of possible fits. In order to gain a quantitative measure of current uncertainties on specific aspects of the parton distributions, only dedicated studies using clearly defined and consistent procedures make scientific sense. Some steps along this line have been taken by the various groups in the exploration of the range of possible small- x behavior [74, 92] (see point (iii) below.) More comprehensive investigations on the ranges for the shape parameters of the parton distributions and the QCD parameter Λ are clearly needed [85]. Indeed, we anticipate the systematic exploration of this multi-dimensional parameter space, utilizing currently available data as well as new data, to be the natural frontier of QCD analysis and phenomenology in the foreseeable future [95].

Generally speaking, the valence quark distributions and the sum of the sea-quark distributions are already very well determined, as they are directly related to the accurate data on DIS structure functions from muon (electron) and neutrino scattering experiments. Figure 4 shows the comparison of these distributions from two recent independent distribution sets.

As far as the other parton distributions are concerned, three areas of uncertainty stand out.

(i) The shape of the gluon distribution: Is it relatively soft or hard in the large- x region? How does it behave at small values of x ?

Some progress has been made in this regard in recent years. High statistics deep inelastic scattering data provide some constraints on the gluon distribution in the region below x of about 0.3, while fixed target lepton-pair and direct photon production experiments probe it in a higher x region, up to 0.6. Figure 5 shows five different recent $\overline{\text{MS}}$ gluon distributions, each evaluated at $Q^2 = 20\text{GeV}^2$. The ABFOW distributions [75] were obtained through a joint fit to the BCDMS deep inelastic data and the WA70 direct photon data. This analysis was intended primarily to demonstrate the utility of including the direct photon data and is not a true global analysis in the sense discussed here. The HMRSB [91] distributions were obtained by fitting these same data and, in addition, data from neutrino deep inelastic scattering and from lepton pair production. The resulting gluon distributions from these two fits are, as

would be expected, quite similar, since the data which most strongly constrains the gluon were the same in each case. The third and fourth gluons comes from the MT global fits [74] to deep inelastic and lepton pair production data, but do not include direct photon data. Set MT-S2 has a suppressed strange quark sea contribution at the initial value of Q_0 (as does HMRSB), and its gluon distribution agrees well with the above two. The MT-S1 set uses an SU(3) symmetric sea; the gluons distribution is somewhat softer than the others above x about 0.25, but is quite similar to them below that value. Finally, the fifth curve shows the result from a recent analysis by the BCDMS group [96] using their data and the recently reanalyzed SLAC data. Both target mass corrections and higher twist terms are included. This new result is very similar to the gluon distributions from the global fits and is not as soft as the results reported earlier by the same group [97]. In order to appreciate that some progress has been made in the determination of the gluon distribution, the spread between these curves should be compared with the much larger differences between, for example, the two gluon distributions in [98] (both are LO and based on the same data sets). Also note the sharp contrast of Figure 5 to similar plots showing a wide spread of the gluon distribution sets often seen in the literature where apples and oranges are all thrown in the same basket.

As more NLO calculations for various large momentum transfer processes have been completed, and as the data have improved, the very soft and very hard gluon distributions appearing in some older parton distribution sets are clearly no longer viable. Furthermore, with new data becoming available soon from both fixed-target and collider experiments, together with improved theoretical understanding of the uncertainties and newly developed tools to control these as discussed in Sec. 4.3, we can expect continued progress on this front. In addition, since jet cross-sections are mostly due to gluon scattering, the increasingly active area of NLO-QCD jet analysis [78] has the promise of placing useful constraints on the gluon distribution, if not directly contributing to its extraction.

The results in Figure 5 also serve to underline another point touched on previously. The only change between the MT-S1 and MT-S2 fits was in the input boundary condition on the strange sea. However, the shape of the resulting gluon distribution was significantly affected. This is indicative of the manner in which the input assumptions can affect the output distributions in unexpected ways. Inclusion of the direct photon data in these fits might have reduced the spread – this is a point currently under investigation.

Another method to get a handle on the gluon distribution is through the longitudinal structure function in deep inelastic scattering, as emphasized by the original papers on QCD. HERA has the potential to finally make this approach realizable [99], especially in the small- x region [30]. We can anticipate strong constraints over a large range of x resulting from the simultaneous comparison of data of this type and new direct photon data from both collider and fixed target experiments.

(ii) Flavor differentiation of the sea quark distributions: Is the strange sea the same as the non-strange ones? Is up-sea the same as the down-sea?

Most LO parton model analyses of existing data on opposite-sign dimuon production in neutrino scattering indicate that the strange-sea content of the nucleon

is suppressed compared to the non-strange sea at a typical Q_0 [100], contrary to the naive expectation of an $SU(3)$ symmetric sea. This feature has been imposed on some of the parton distribution sets obtained in global fits, as mentioned above. However, because of the significant gluon-sea-quark mixing at moderate scale Q , (see Sec. 6), the gluon contribution to this process can be rather large, and hence affect this conclusion. The on-going analysis of currently available data on dimuon production will incorporate the important NLO contributions [101], thus allowing a much more meaningful determination of the strange quark distribution defined in a specific renormalization scheme. In the future, the planned next-generation neutrino experiment at Fermilab expects to measure one order of magnitude more dimuon events [102]. This will allow a definitive QCD analysis of the charm production process.

The new results from NMC[70] raised doubt whether the \bar{u} and \bar{d} distributions are the same, as is usually assumed. In order to settle this issue, it is desirable to exploit constraints imposed by different sources, such as lepton-pair production and forward-backward-asymmetry in W production in addition to deep inelastic scattering. The experimental accuracy for these processes is improving, and careful combined analysis should allow the determination of the limits on the breaking of flavor $SU(2)$ symmetry of the sea.

Significant advances in flavor-differentiation of the sea-quarks in general can be achieved with a definitive experiment on neutrino scattering which will allow the separate measurement of neutrino- and anti-neutrino structure functions — by way of the y -distributions of the respective cross-sections. (Currently, due to insufficient statistics, the structure functions are obtained from the sum and difference of the two cross-sections supplemented by assumed relations among the structure functions [26].) This will allow the determination of more linear combinations of parton distribution functions, and hence provide the necessary information to unambiguously extract parton distributions of all flavors. Such an experiment has been proposed at Fermilab for the 1990's [102]. It should crown the remarkable achievement of the line of DIS experiments which have always played the central role in the QCD parton framework.

(iii) Small- x behavior of parton distribution functions: What is the range of possible small- x behavior? Is it possible to calculate the “small- x evolution” of parton distributions?

Predictions on cross-sections for standard model and new physics processes at the next generation colliders depend critically on the behavior of the parton distribution functions at small- x values beyond current measurements. Current uncertainty on this front is rather large. A systematic phenomenological study of the allowed range of small- x behavior, with current data as constraints, using a generalized initial distribution function containing a logarithm factor ($P(x)$ of Eq. (18)) in addition to the traditional power-law reveal an effective power-law exponent in the range $(0, -0.45)$ at $Q = 2.5$ GeV converging to the much narrower range of $(-0.58, -0.63)$ at $Q = 10^4$ GeV. (cf. Figure 4 of [25]) In the immediate future, the DIS experiments NMC[70] and E665[103] will extend the x -range somewhat before the much anticipated new results from HERA become available. From hadron collider experiments, we expect low-mass lepton-pair production to be particularly sensitive to small- x behavior of the parton distribution functions [104]. If the rapidity range of these measurements

can be expanded beyond the central region, x -values below 10^{-3} can be effectively probed. Data from the Tevatron on this process will soon be available for analysis.

As briefly discussed in Sec. 3.3, much theoretical effort is currently devoted to gaining more understanding of the small- x behavior and to develop methods to calculate the parton distributions in this region. Of particular interest are possible generalizations of the familiar Q -evolution of parton distributions in other directions on the x - Q plane — “vertically” toward small- x or “diagonally” toward large $s(\propto Q^2/x)$ based on different resummations in these varied regions. Initial numerical studies of the currently available formalisms indicate remarkable (and unexpected) agreement between the various resummation approaches [105]. This lends more credibility to the existing calculations based on conventional twist-2 QCD, but does not yet provide useful predictive power toward small- x . Theoretical progress in this direction in the near future would be most opportune, as comparison with new experimental results from HERA should provide tests of QCD in yet another dimension.

8 Conclusion

The determination of the universal parton distribution functions in the QCD framework is intimately linked to all aspects of rigorous tests of the Standard Model: the effort to extract more precise distribution functions from an ever wider range of processes becomes inseparable from efforts to check the consistency and to push the limit of the SM in order to discover signs of new physics. At the same time, knowledge of these distribution functions allows us to make predictions on anticipated physics measurements at much higher energy regimes than achievable at present. As described above, much challenging work, both theoretical and experimental, remains to be done. With regard to global analyses, several near-term goals include the following: (i) inclusion of additional direct photon data to further constrain the gluon distribution with attention being paid to the question of how the scale dependence affects the resulting distributions and also the effects of isolation cuts and the bremsstrahlung contribution; (ii) further study of the flavor dependence of the sea distributions and the inclusion of neutrino produced dimuon data in the analyses; (iii) further study of the theory and phenomenology of the small- x regime and the inclusion of new results from HERA for both the longitudinal and transverse structure functions as they become available; (iv) continued study of appropriate methods for treating the statistical and systematic errors of the different data sets; and (v) systematic investigation of the range of uncertainty of the QCD parameters, including the shape parameters of the uncalculable “initial distributions” and of possible experiments to reduce these uncertainties. With coordinated efforts on all these fronts, QCD analysis and phenomenology is entering an era of unprecedented precision, similar (but of course not yet comparable) to electroweak phenomenology. It is a very rich field, and it will continue to play a central role in high energy physics in the context described above.

References

- [1] Langacker, P., in the proceedings of the *XXIVth* International Conference on High Energy Physics, ed. R. Kotthaus and J.H. Kühn, p. 190. Berlin Heidelberg: Springer-Verlag (1989).
- [2] Altarelli, G., *Annu. Rev. Nucl. Part. Sci.* 39: 357 (1989).
- [3] Geesaman, D.F., Morfin, J., Sazama, C., Tung, W.K., eds. *Proceedings of Workshop on Hadron Structure Functions and Parton Distributions*, Singapore: World Scientific, 500 pp.(1990).
- [4] Collins, J.C., Soper, D.E. *Annu. Rev. Nucl. Part. Sci.* 37: 383 (1987).
- [5] Collins, J.C., Soper, D.E., Sterman, G. in *Perturbative Quantum Chromodynamics*, ed. A. Mueller. Singapore: World Scientific (1989).
- [6] Owens, J.F., *Rev. Mod. Phys.* 59:465 (1987).
- [7] Tung, W.K., p.18 in [3].
- [8] T. Appelquist and J. Carazzone, *Phys. Rev.* D11:2856 (1975).
- [9] Collins, J.C., Wilczek, F., Zee, A. *Phys. Rev.* D18 , 242 (1978); Collins, J.C., Tung, W.K. *Nucl. Phys.* B278, 934 (1986); See also Marciano, W. *Phys. Rev.* D29, 580 (1984).
- [10] Gribov, L.V., Lipatov, L.N., *Sov. J. Nucl. Phys.* 15: 78 and 1218 (1972).
- [11] Altarelli, G., Parisi, G., *Nucl. Phys.* B126:298 (1977).
- [12] Floratos, E.G., Ross, D.A., Sachrajda, C.T., *Nucl. Phys.* B129: 66(1977); erratum, *Nucl. Phys.* B139: 545(1978); Floratos, E.G., Lacaze, R., Kounnas, C., *Phys. Lett.* 98B: 89(1981).
- [13] Gonzalez-Arroyo, A., Lopez, C., Yndurain, F.J., *Nucl. Phys.* B153:161(1979); B166: 429(1980).
- [14] Curci, G., Furmanski, W., Petronzio, R., *Nucl. Phys.* B175: 27(1980); Furmanski, W., Petronzio, R., *Phys. Lett.* 97B: 438 (1980).
- [15] Herrod, R.T., Wada, S., *Phys. Lett.* 96B:195 (1980); Herrod, R.T., Wada, S., Webber, B.R., *Z. Phys.* C9:351 (1981).
- [16] Hamberg, R., van Neerven, W.L., University of Leiden report INLO-PUB-13/91.
- [17] Tung, W.K. *Phys. Rev. Lett.*, 35:490 (1975); and *Phys. Rev.* D12:3613 (1975).
- [18] Collins, J.C., Qiu, Jianwei, *Phys. Rev.* D39: 1398(1989).

- [19] Bartel, J. ed. *Proceedings of Workshop on Small- x Behavior of Parton Distributions*, Amsterdam: North Holland (1991).
- [20] Lipatov, L.N., *Sov. J. Nucl. Phys.*, 23:338 (1976); Kuraev, E.A., Lipatov, L.N., & Fadin, V.S., *Sov. Phys. JETP* 45:199 (1978).
- [21] Collins, J.C., Ellis, K., p.80 in [19].
- [22] Gribov, L.V., Levin, E.M., Ryskin, M.G. *Phys. Rep.* 100: 1 (1982); Levin, E.M., Ryskin, M.G. *Phys. Rep.* 189:269 (1990); Levin, E.M., Ryskin, M.G., p.92 in [19]; and Levin, E.M., *Proceedings of the EP-HEP 91 Conference, Geneva* (DESY Preprint 91-110, to be published).
- [23] Mueller, A.H., Qiu, Jianwei. *Nucl. Phys.* B268: 427 (1986); Mueller, A.H., p.125 in [19].
- [24] Collins, J.C., in *Physics Simulations at High Energy*, V. Barger, T. Gottschalk, F. Halzen, eds. p.265. Singapore: World Scientific (1987).
- [25] Tung, W.K., p.55 in [19].
- [26] Wu-Ki Tung et al, in *Proceedings of the 1988 Summer Study on High Energy Physics in the 1990's*, S. Jenson ed., p. 305. Singapore: World Scientific, (1989).
- [27] Bardeen, W.A., Buras, A.J., Duke, D.W., Muta, T., *Phys. Rev.* D18:3998 (1978).
- [28] Altarelli, G., Ellis, R.K., Martinelli, G., *Nucl. Phys.* B143:521 (1978).
- [29] Duke, D.W., *et al.*, *Phys. Rev.* D25:71 (1982); Devoto, A., *et al.*, *Phys. Rev.* D30:541 (1984).
- [30] Cooper-Sarkar, A.M., *et al.*, *Z. Phys.* C39:281 (1988).
- [31] Drell, S., Yan, T.M., *Phys. Rev. Lett.* 25:316 (1970).
- [32] Altarelli, G., Ellis, R.K., Martinelli, G., *Nucl. Phys.* B157:461 (1979).
- [33] Kubar, J., Le Bellac, M., Meunier, J.L., Plaut, G., *Nucl. Phys.* B175:251 (1980).
- [34] T. Matsuura, R. Hamberg, W.L. van Neerven, *Nucl.Phys.* B345:331, 1990.
- [35] Sterman, G., *Phys. Lett.* 179B: 281 (1986); *Nucl. Phys.* B281: 310 (1987); and p. 423 in [3]. See also S. Catani, Trentedue, L., *Nucl. Phys.* B327:323 (1989).
- [36] For example, talk in *Workshop on Hadron Structure Functions and Parton Distributions*, [3].
- [37] Altarelli, G. *et al.*, *Nucl. Phys.* B246:12 (1984).
- [38] Collins, J.C., Soper, D., Sterman, G., *Nucl. Phys.* B250:199 (1985).

- [39] Arnold, P.B., Reno, M.H., *Nucl. Phys.* B319: 37 (1989); erratum B330: 284 (1990); Arnold, P.B., Kauffman, R.P., *Nucl. Phys.* B349: 381 (1991).
- [40] Aurenche, P., Douiri, A., Baier, R., Fontannaz, M., Schiff, D., *Phys. Lett.* 140B:87 (1984).
- [41] Berger, E.L., Braaten, E., Field, R.D., *Nucl. Phys.* B239:52 (1984).
- [42] Camilleri, L., p. 203 in the proceedings of the 19th *Symposium on Multiparticle Dynamics*, Arles, France, 1988.
- [43] Baer, H., Ohnemus, J., Owens, J.F., *Phys. Rev.* D42:61 (1990).
- [44] Baer, H., Ohnemus, J., Owens, J.F., *Phys. Lett.* B234:127 (1990).
- [45] AFS Collab., Åkesson, T. et al., *Sov. J. Nucl. Phys.* 51:836 (1990).
- [46] Koller, K., Walsh, T.F., Zerwas, P.M., *Z. Phys.* C2:197 (1979).
- [47] Berger, E.L., Qiu, J., *Phys. Lett.* B248: 371 (1990); *Phys. Rev.* D44: 2002 (1991).
- [48] Berger, E.L., Qiu, J., private communication.
- [49] Aivazis, M.G., Olness F., & Tung, W.K, *Phys. Rev. Lett.* 65:2339 (1990).
- [50] Gottschalk, T., *Phys. Rev* D23: 56 (1981).
- [51] van der Bij, J.J., van Oldenborgh, G.J., *Z. Phys.* C51: 477 (1991).
- [52] Olness, F.I., and Tung, W.K, *Nucl. Phys.* B308:813 (1988).
- [53] Nason, P., Dawson, S., Ellis, R.K., *Nucl. Phys.* B303: 607 (1988); B327, 49 (1989); erratum, B335: 260 (1990).
- [54] Beenakker, W., et al., *Phys. Rev.*, D40:54 (1989); *Nucl. Phys.*, B351:507 (1991); and Laenen, E., et al., *Nucl. Phys.*, Stony Brook report ITP-SB-91-14.
- [55] Ellis, S.D., Kunszt, Z., Soper, D.E., *Phys. Rev.* D40:2188 (1989); *Phys. rev. Lett.* 62: 726 (1989); 64: 2121 (1990).
- [56] Aversa, F., Greco, M., Chiapetta, P., Guillet, J.Ph., *Z. Phys.* C46: 253 (1990); *Nucl. Phys.* B237: 105 (1989); *Phys. Lett.* 210B: 225 (1988); 211B: 465 (1988).
- [57] Mangano, M.L., Parke, S.J., *Phys. Rep.* 200:301 (1991)
- [58] Giele, W.T., Glover, E.W.N., Kosower, D.A., FNAL report FERMILAB-CONF-91-243-T, FERMILAB-CONF-91-274-T (1991).
- [59] Bern, Zvi, and Kosower, D., FNAL report FERMILAB-91-111-T, and detailed references cited therein.
- [60] Schuler, G., et al., in Proceedings of Snowmass 90 Workshop.

- [61] Mishra, S., Sciulli, F., *Annu. Rev. Nucl. Part. Sci.* **39**: 259-310 (1989).
- [62] BCDMS Collaboration (A.C. Benvenuti, *et.al.*), *Phys.Lett.*, **B189**:483 (1985); *ibid*, **B195**:91 (1987); *ibid*, **B223**:485 (1989); *ibid*, **B237**:592 (1990); *ibid*, **B237**:599 (1990).
- [63] CHARM Collaboration (J.V. Allaby, *et.al.*), *Z. Phys.*, **C36**:611 (1987).
- [64] CDHSW Collaboration (J.P.Berge *et.al.*), *Z. Phys.*, **C49**, 187 (1991).
- [65] FMM Collaboration, Cobau, W., Report at DPF91 conference, Vancouver, August (1991).
- [66] CCFR Collaboration (Mishra, S.R. *et al.*), Nevis report NEVIS-1466 (1992).
- [67] SLAC Experiments (Whitlow, L.W., *et.al.*), report SLAC-PUB-5442 (1991); *Phys.Lett.* **B250**:193 (1990).
- [68] K. Bazizi, S.J. Wimpenny, and T. Sloan, in *Proceedings of the 25th International Conference on High Energy Physics*, Singapore, (1990).
- [69] For the controversy, see R. Mount in *Proceedings of XXIV International Conference on High Energy Physics*, Munich, 1988, R. Kotthaus Ed., Springer, 1989; For the resolution, see papers by Bodek, Milsztajn and Wimpenny in [3] and in *Proceedings of the 1991 International Symposium on Lepton and Photon Interactions at High Energies*, Geneva (to be published).
- [70] Amaudruz, P., *et al.* *Z. Phys.* **C 51**:387 (1991).
- [71] Roberts, R.G., Whalley, M.R., *J. Phys.* **G17**: 1 (1991).
- [72] For a review, see Rutherford, J. P., p. 234 in [3].
- [73] C.N. Brown *et.al.*, *Phys. Rev. Lett.* **63**:2637 (1989).
- [74] Morfin, J.G., and Tung, W.K., *Z. Phys.* **C52**:13 (1991).
- [75] Aurenche, P., Baier, R., Fontannaz, M., Owens, J.F., Werlen, M., *Phys. Rev.* **D39**:3275 (1989).
- [76] Bonensini, M., *et al.*, *Z. Phys.* **C38**: 371 (1988).
- [77] E706 (Alverson, G., *et.al.*) Fermilab report Fermilab-Pub-91/212 (1991).
- [78] CDF Collaboration. For references, see Huth, J., Fermilab report Fermilab-Conf-91/223-E (1991)
- [79] E.L. Berger (Argonne), F. Halzen, C.S. Kim, S. Willenbrock, *Phys.Rev.* **D40**:83, 1989, Erratum, *ibid*, **D40**:3789 (1989).

- [80] R.K. Ellis, W. Furmanski and R. Petronzio, *Nucl. Phys.* **B207**:1 (1982); **B212**:29 (1983).
- [81] Qiu, J.W. and Sterman, G, *Nucl.Phys.*, **B353**:105 (1991); **B353**:137 (1991).
- [82] Milsztajn, A., p.76 in [3]; Virchaux, M., p.124 in [3].
- [83] Devoto, A., Duke, D.W., Owens, J.F., Roberts, R.G. *Phys. Rev.* D27: 508 (1983).
- [84] Arneodo, M. et.al., *Nucl. Phys.* **B331**:1 (1990).
- [85] Martin A.D., Roberts R.G., Stirling W.J., *Phys. Rev.* D43:3648 (1991).
- [86] Glück, M., Reya, E., Vogt, A. Dortmund report DO-TH 91/07 *Z. Phys.*, in press.
- [87] Reya,E. Dortmund report DO-TH 91/09, to appear in the proceedings of the *Workshop on High Energy Physics Phenomenology II*, Calcutta, January 1991, to be published by World Scientific.
- [88] Duke, D.W., Owens, J.F., *Phys. Rev.* D30: 49 (1984); Eichten, E., et al., *Rev. Mod. Phys.* 56: 579 (1984) and erratum 58: 1065 (1986); Glück, M., Reya, E., Hoffmann, E., *Z. Phys.* C13: 119 (1982).
- [89] Diemoz, M., et al., *Z. Phys.* C39: 21 (1988).
- [90] Martin, A.D., Roberts, R.G., Stirling, W.J., *Phys. Rev.* D37: 1161 (1988); *Mod. Phys. Lett.* **A4**: 1135 (1989).
- [91] Harriman, P.N., Martin, A.D., Roberts, R.G., & Stirling, W.J., *Phys. Rev.* **D42**, 798 (1990).
- [92] Kwiecinski, J., Martin A.D., Roberts, R.G., Stirling, W.J., *Phys.Rev.*, **D42**:3645 (1990).
- [93] H. Plathow-Besch, "PDFLIB: Structure Functions and α_s Calculation User's Manual" CERN-PPE, 1991.03.21, W5051 PDFLIB.
- [94] Owens, J.F., *Phys. Lett.* B266: 126 (1991).
- [95] A long term project involving 12 theorists and experimentalists from 8 institutions – Coordinated Theoretical/Experimental Project on Quantitative QCD Phenomenology and Tests of the Standard Model (CTEQ) – has recently been formed to address the full range of theoretical and phenomenological problems in a systematic and consistent fashion.
- [96] Virchaux, M., Milsztajn, A., Saclay report DPhPE 91-08 (1991).
- [97] Benvenuti, A.C., et al., *Phys. Lett.* B195: 97 (1987).

- [98] Duke, D.W., Owens, J.F., *Phys. Rev. D* **30**: 49 (1984).
- [99] Proceedings of HERA *Workshop*, ed. Peccei, R.D., DESY (1988).
- [100] See C. Foudas, *et.al.*, *Phys. Rev. Lett.* **64**:1207 (1990) and references cited therein.
- [101] Private communications: Brock, R., (FMM) and Shaevitz, M., (CCFR).
- [102] Mishra, S., "A Next Generation Neutrinoexperiment At FNAL Tevatron", Nevis Report #1435 (1991).
- [103] M.R. Adams *et al.*, *Nucl. Inst. and Meth.* **A291**:533 (1990).
- [104] Olness, F., and Tung, W.K. , p. 523 in *From Colliders to Super Colliders*, ed. V. Varger and F. Halzen, World Scientific (1987).
- [105] Krawczyk, M., p. 64 in [19]; Badelek, B., *et.al.*, DESY report DESY- 91-124 (1991).

Figure Captions

1. (a) α_s and (b) Λ_{QCD} as functions of μ and n_f^{eff} .
2. Comparison of parton distributions defined in the DIS and \overline{MS} schemes: (a) the strange quark; and (b) the gluon. Two representative distributions from the recent analyses of the HMRS and MT groups are shown. Conversion of one scheme to the other is done according to the text.
3. Comparison of representative data from the BCDMS experiment with predictions from three recent NLO parton distribution sets: DFLM, HMRSB, and MT-S2.
4. Comparison of the valence distributions from the HMRSB and MT-S2 sets of parton distribution functions.
5. Comparison of several different \overline{MS} gluon distributions: ABFOW [75] (solid), HMRSB [91] (dashed), MT-S1 [74] (dash-short dash), MT-S2 [74] (dash-dot), and BCDMS [96] (dotted).

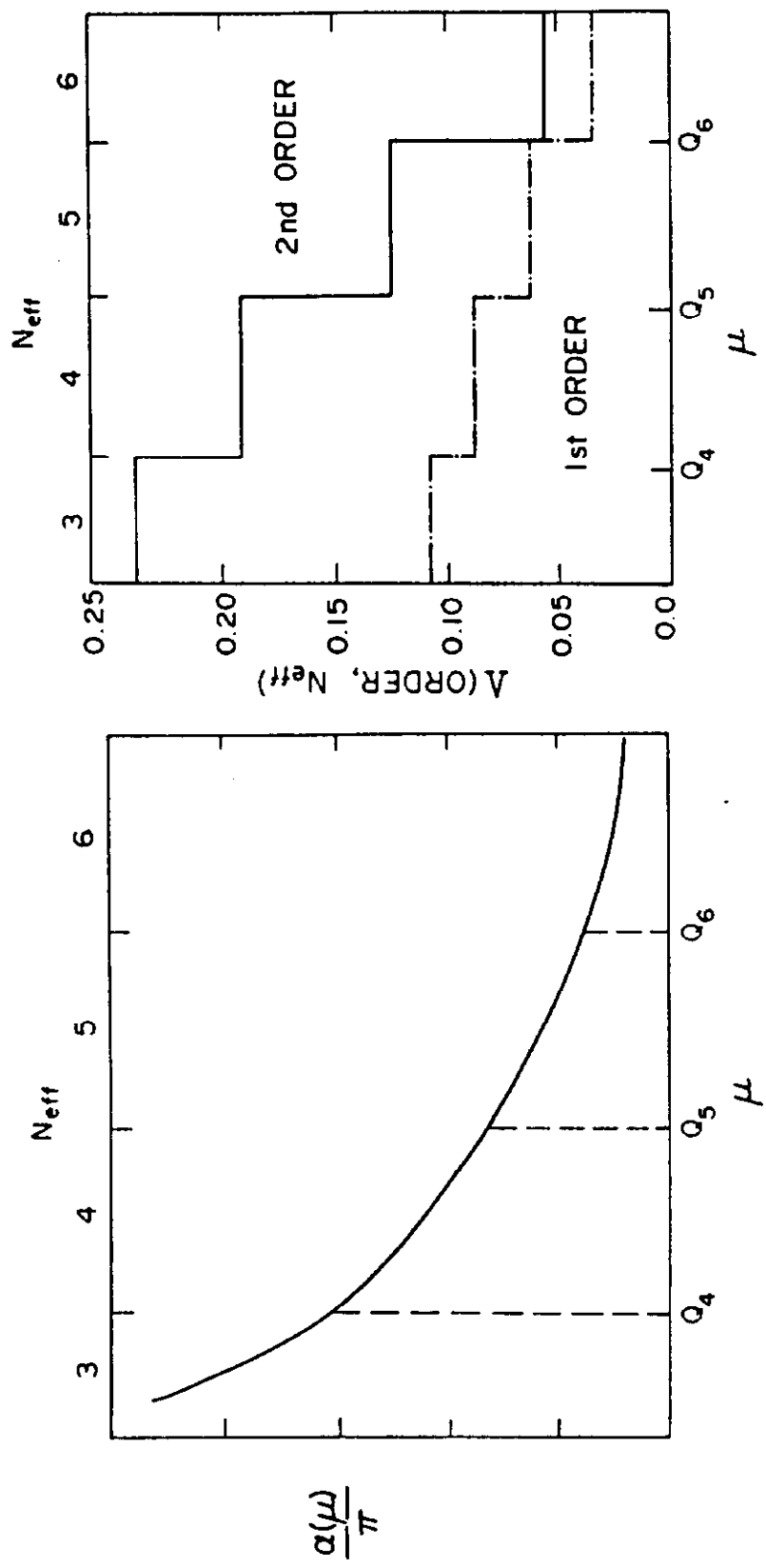


Fig. 1

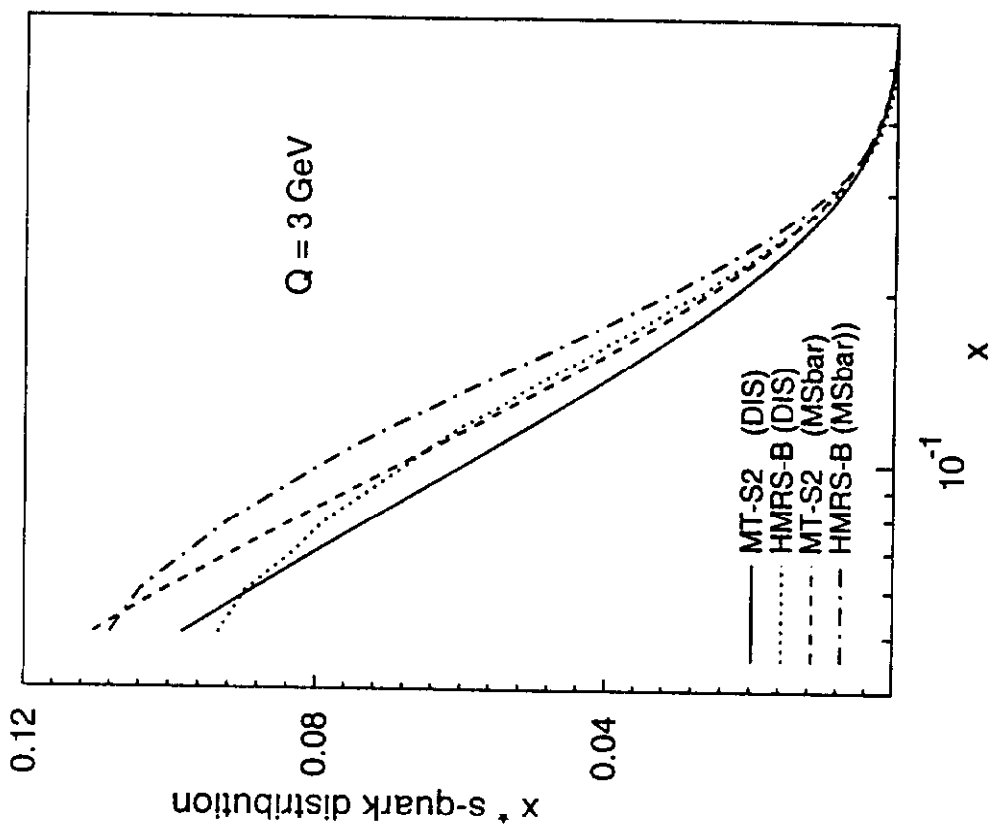
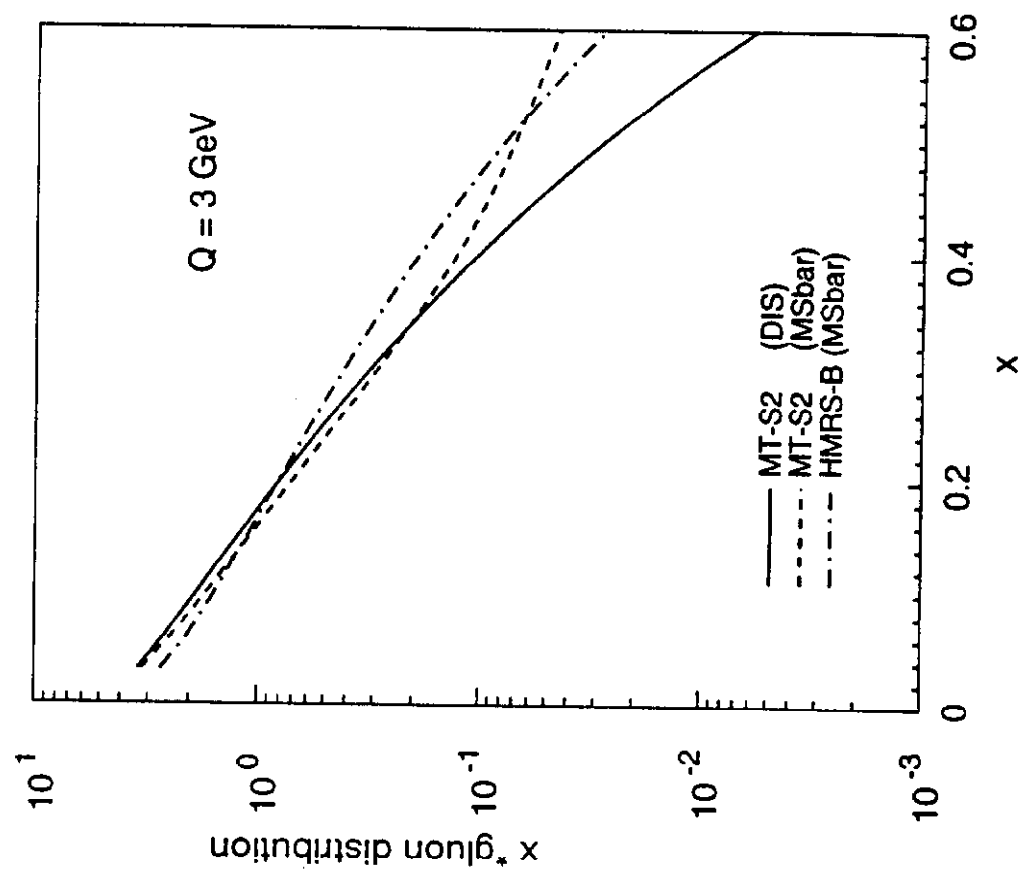
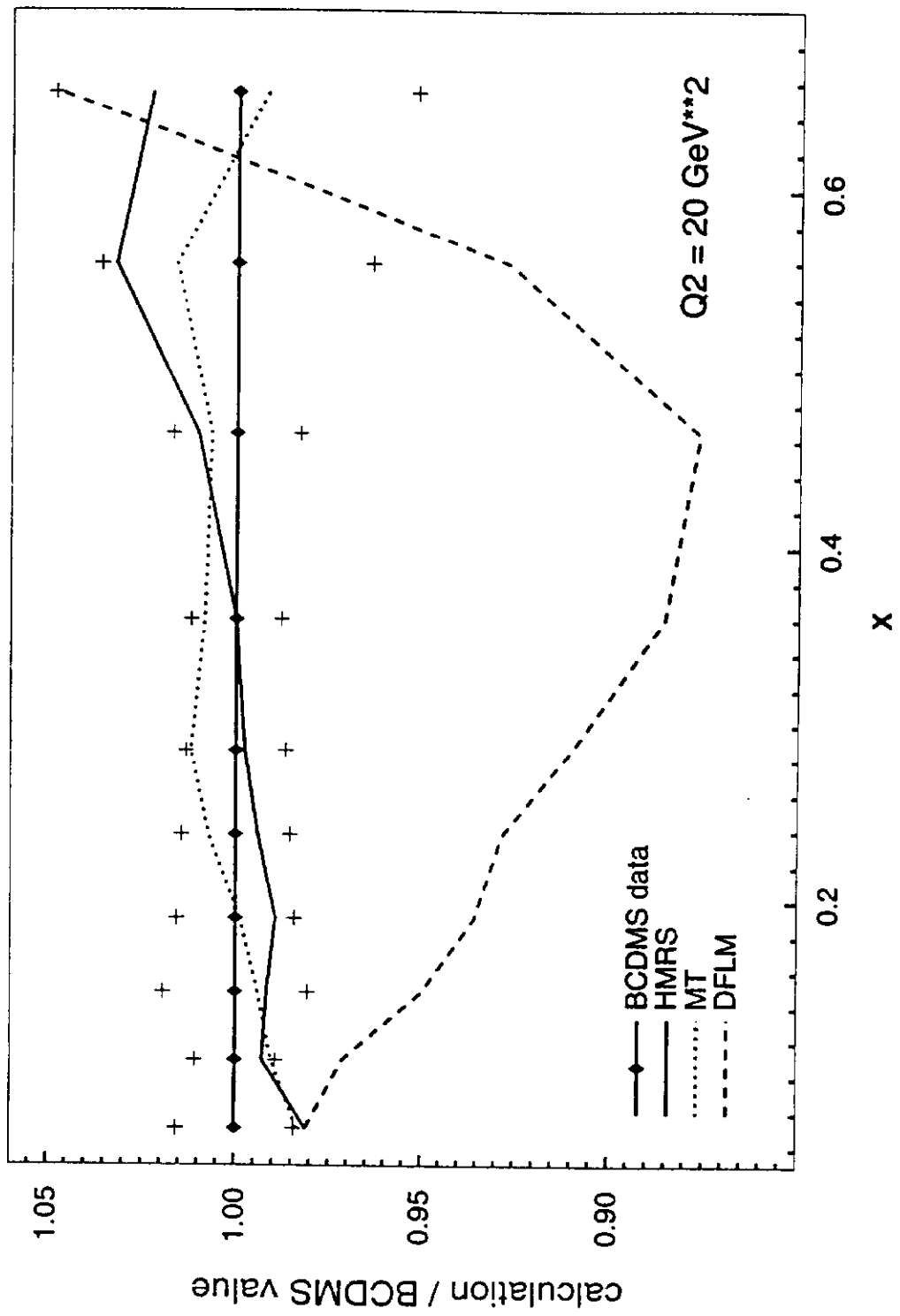


Fig. 2.

Fig.3



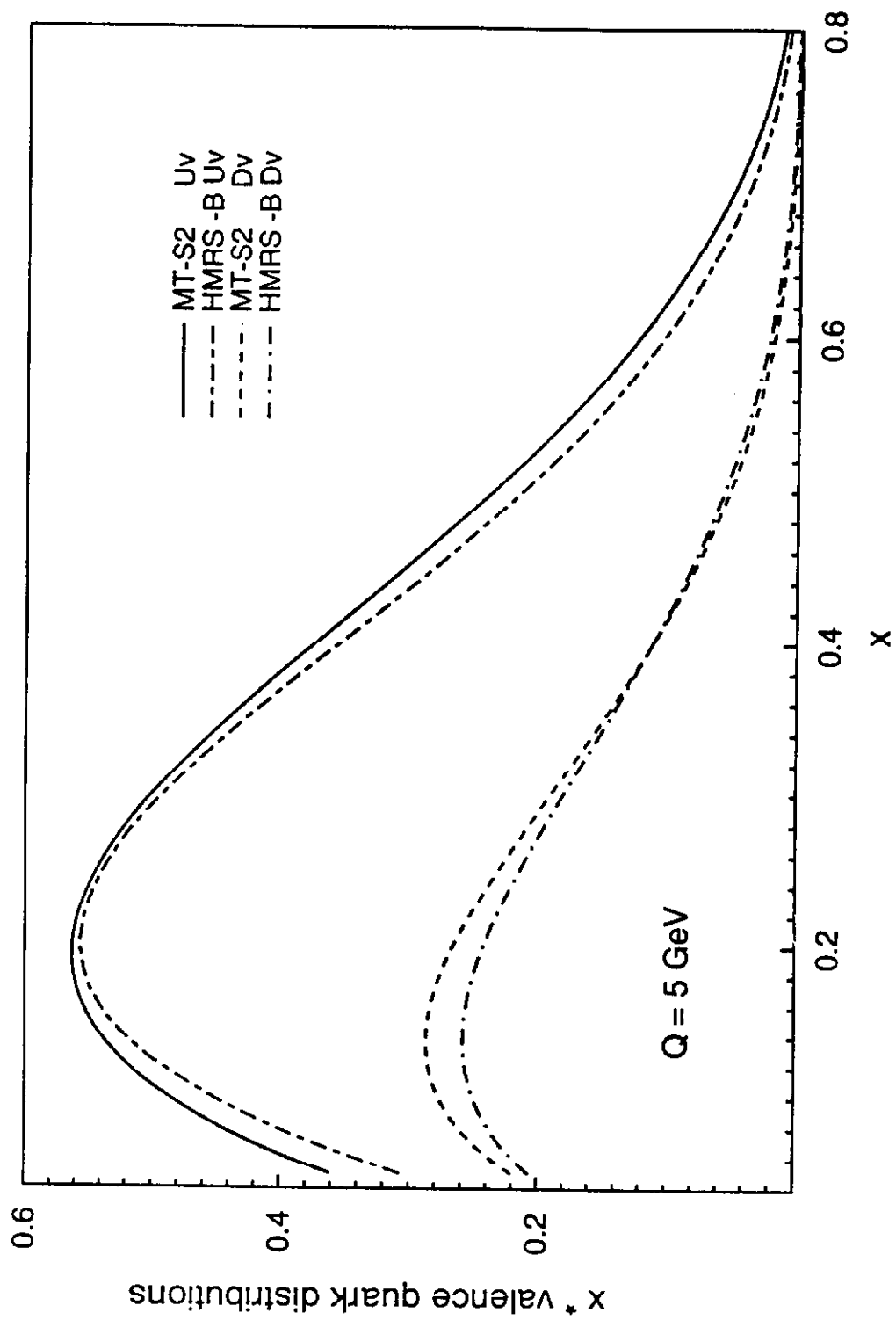


Fig. 4

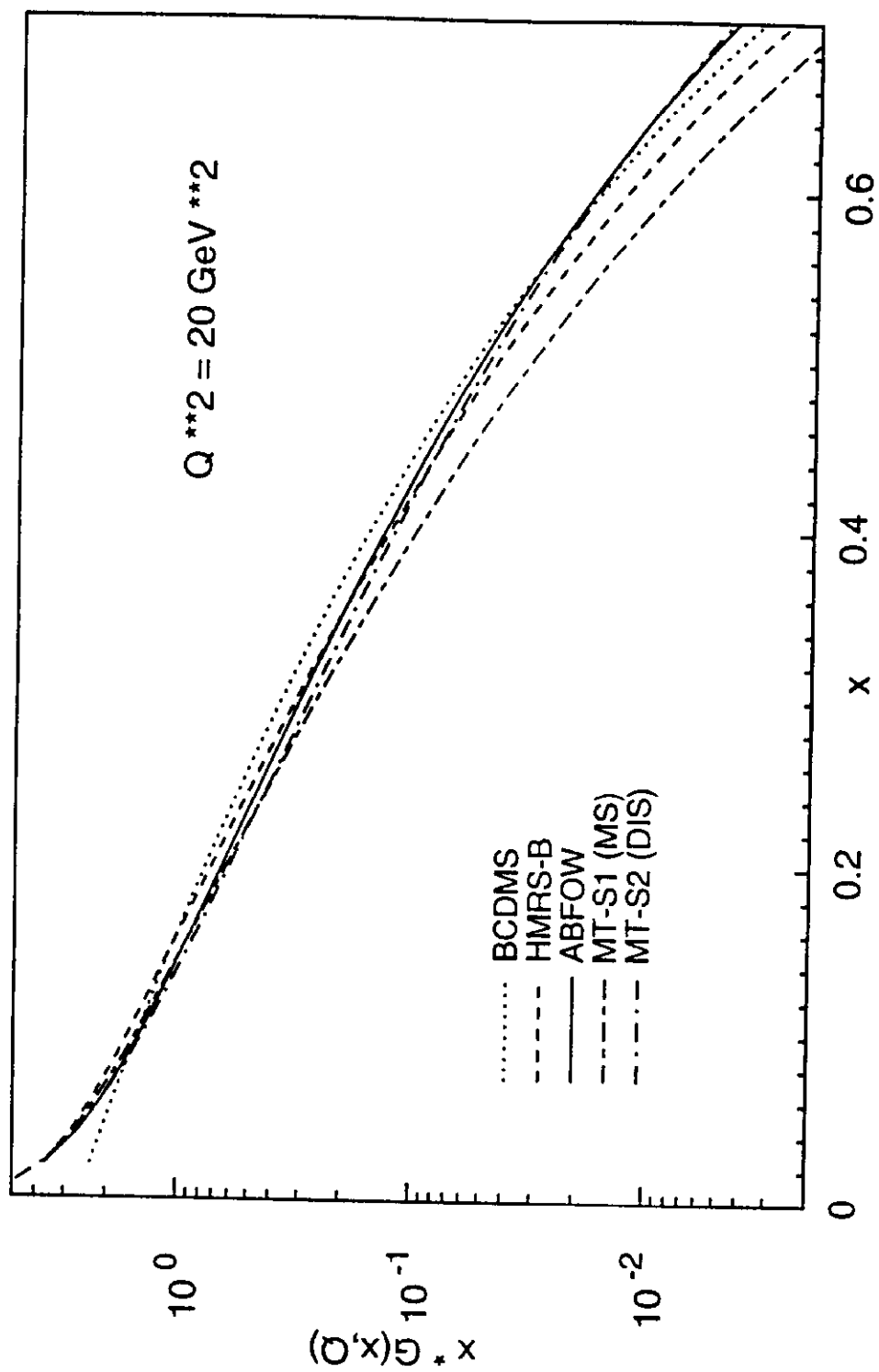


Fig. 5